

NACA TN 4223 10563

TECH LIBRARY KAFB, NM
006648

NATIONAL ADVISORY COMMITTEE FOR AERONAUTICS

TECHNICAL NOTE 4223

RELATION OF JOURNAL BEARING PERFORMANCE TO
MINIMUM OIL-FILM THICKNESS

By F. W. Ocvirk and G. B. DuBois
Cornell University



Washington
April 1958

TECHNICAL LIBRARY
AFL 2911



0066848

TECHNICAL NOTE 4223

RELATION OF JOURNAL BEARING PERFORMANCE TO
MINIMUM OIL-FILM THICKNESS

By F. W. Ocvirk and G. B. DuBois

SUMMARY

The minimum thickness of the oil film is used as a basic variable in performance curves of plain journal bearings under a steady load. Analytical curves based on the short-bearing solution and the solution of Cameron and Wood are compared with experimental data from four published sources.

The load capacity and the predicted film thickness at the hook point of the friction curves are shown to correlate with the peak-to-valley values of surface roughness when misalignment is absent. The effect of bearing-clearance changes on the friction power loss, the film thickness, and the peak pressure in the oil film is shown by analytical curves.

INTRODUCTION

The minimum thickness of the oil film offers definite advantages as a basic variable for plotting the performance of plain journal bearings. First, in contrast with the more commonly known curves with eccentricity ratio as a variable, the curves with minimum oil film thickness as a variable are more directly related to the factors which evidently limit the load capacity, such as the roughness of the bearing surfaces and the misaligning effects of elastic deflection. Second, the minimum film thickness may be expressed in nondimensional forms which avoid introducing the bearing clearance into the variable, so that the effect of varying the bearing clearance may be more easily shown.

The value of the minimum film thickness as a basic variable has been recognized by Demmison (ref. 1) and by Boyd and Raimondi (ref. 2) who present tables and curves obtained from solutions based on leakage factors determined by the electric analog method of Kingsbury (ref. 3) and Needs (ref. 4).

The analysis of bearing performance would be greatly simplified if exact solutions were available in equation form because of the facility with which equations indicate suitable parameters and methods of plotting experimental data. However, most of the exact solutions consist essentially of coordinates of data points.

While the Ocvirk short-bearing approximation (ref. 5) is considered technically exact only for bearings of infinitely small l/d ratio, the results given by this method are the closest approximation so far found in equation form for bearings having values of l/d up to 1. The curves obtained have been especially useful as a basis for comparing other analytical and experimental data. The exact analytical and experimentally determined curves are useful for bearings having values of l/d up to 1, and may be extended to larger values of l/d by the device of neglecting the l/d term in the load number in the charts related to load capacity and film thickness (ref. 6). Since the load number is equivalent to the reciprocal of $S(l/d)^2$, neglecting the l/d term is equivalent to reverting to the Sommerfeld number S which is considered exact for bearings of infinite l/d ratio.

The purpose of the present report is to derive equations including the minimum film thickness h_m as a variable from the short-bearing approximation and to illustrate how the resulting parameters may be used for plotting experimental and analytical data.

In this report the curves form a basis for comparison of exact analytical solutions and experimental data from four published sources. The solutions of Cameron and Wood (ref. 7) were obtained by the relaxation method and are considered mathematically exact, but they were obtained essentially from point data rather than from equations. The experimental data shown were given by Kreisle (ref. 8), by Dayton, Allen, Fawcett, Miller, and Grimble (ref. 9), by Burwell, Kaye, Van Nymegen, and Morgan (ref. 10), and in a previous report on the present investigation (ref. 6).

The resulting curves illustrate the relation of film thickness and bearing clearance to journal-bearing performance, including film load capacity, friction, and peak-pressure ratio. The methods of obtaining the various curves are described in the following discussion using the symbols shown in figure 1 and the list of symbols. Figures 2 and 3 summarize the relation of load capacity to film thickness. Figure 3 is of special interest as it shows the analytical effect of large changes of bearing clearance on the load capacity for several values of film thickness. Unfortunately, no experimental data of sufficient range of clearance change could be found for comparison.

Figure 4 is also of special interest since it shows a remarkably close correlation between the predicted values of minimum film thickness at operating conditions near the hook point of friction curves with the sum of the peak-to-valley roughnesses of the two surfaces. A rigorous interpretation of the meaning of the root-mean-square values of surface roughness was necessary using Tarasov's conversion factors (ref. 11) to convert root-mean-square readings to "predominant-peak" roughness.

The use of h_m as a variable is also extended to curves of journal friction in figure 5 which show that the power loss passes through a minimum as the bearing clearance is increased from a small value. While these curves are analytical, they are based on curves for which experimental support is shown in reference 6.

This investigation was conducted at Cornell University under the sponsorship and with the financial assistance of the National Advisory Committee for Aeronautics.

SYMBOLS

Dimensional quantities:

c_d	diametral bearing clearance, in.
d	bearing diameter, in.
e	eccentricity of journal and bearing axes, in.
e_h	lateral component of eccentricity, $e \sin \phi$, in.
F	friction force, lb
F_b	friction force on stationary bearing surface, lb
F_j	friction force on rotating journal surface, lb
F_0	Petroff friction force at zero eccentricity, $2\pi^2\mu N' \omega d(d/c_d)$, lb
ΔF	friction force or torque due to couple formed by central load and lateral component of eccentricity, lb
h_m	minimum film thickness at point of closest approach, in.

l	bearing length, in.
N'	journal speed, rps
P	applied central load on bearing, lb
p	unit load on projected area, P/l_d , lb/sq in.
P_{max}	peak pressure in fluid film, lb/sq in.
T	couple formed by central load and lateral component of eccentricity, in-lb
ΔT	torque equal to couple formed by central load and lateral component of eccentricity, in-lb
θ_{max}	angle measured from location of maximum film thickness to location of peak pressure in fluid film, deg
ϕ	attitude angle, angle between load line and line of centers of journal and bearing, deg
μ	viscosity of fluid, reyns
Nondimensional quantities:	
c_d/d	diametral-clearance ratio
C_n	capacity number
l/C_n	load number, $\frac{P}{\mu N'} \left(\frac{c_d}{d}\right)^2 \left(\frac{d}{l}\right)^2$
$\frac{F/l_d}{\mu N'}$	friction number
f	coefficient of friction, F/P
h_m/d	minimum-film-thickness ratio
k	peak-pressure ratio, P_{max}/P
l/d	length-diameter ratio
n	eccentricity ratio, $2e/c_d$

$\frac{p}{\mu N'} \left(\frac{d}{l}\right)^2$ film capacity number

S Sommerfeld number, $\frac{\mu N'}{p} \left(\frac{d}{c_d}\right)^2$

ANALYTICAL CURVES

The relationship between load capacity and minimum film thickness as shown in figure 2 may be analytically derived from the basic equation of the short-bearing approximation (ref. 5) which equates the load number $1/C_n$ to a function of eccentricity ratio n :

$$1/C_n = \frac{p}{\mu N'} \left(\frac{c_d}{d}\right)^2 \left(\frac{d}{l}\right)^2 = \frac{\pi n}{(1-n^2)^2} [\pi^2(1-n^2) + 16n^2]^{1/2} \quad (1)$$

Equation (1) is shown plotted in the curves of figures 6 and 7. In this form it is not readily apparent that the bearing clearance c_d may be eliminated from the equation. However, the minimum film thickness h_m and diametral bearing clearance c_d are interrelated with eccentricity ratio as follows:

$$\frac{h_m}{c_d/2} = (1-n) \quad (2)$$

Derivation of h_m Parameter

The $(1-n^2)^2$ term of equation (1) may be factored algebraically so that equation (1) may be rewritten as follows:

$$\frac{p}{\mu N'} \left(\frac{c_d}{d}\right)^2 \left(\frac{d}{l}\right)^2 = \frac{\pi n}{(1-n)^2(1+n)^2} [\pi^2(1-n^2) + 16n^2]^{1/2} \quad (3)$$

Substitution of equation (2) in equation (3) gives:

$$\frac{p}{\mu N'} \left(\frac{c_d}{d}\right)^2 \left(\frac{d}{l}\right)^2 = \left(\frac{c_d}{h_m}\right)^2 \frac{\pi n}{4(1+n)^2} [\pi^2(1-n^2) + 16n^2]^{1/2}$$

$$\frac{p}{\mu N'} \left(\frac{h_m}{d} \right)^2 \left(\frac{d}{l} \right)^2 = \frac{\pi n}{4(1+n)^2} \left[\pi^2(1-n^2) + 16n^2 \right]^{1/2}$$

$$\frac{p}{\mu N'} \left(\frac{h_m}{d} \right)^2 \left(\frac{d}{l} \right)^2 = f(n) \quad (4)$$

in which

$$f(n) = \frac{\pi n}{4(1+n)^2} \left[\pi^2(1-n^2) + 16n^2 \right]^{1/2}$$

Equation (4) may be rewritten:

$$\frac{p}{\mu N'} \left(\frac{d}{l} \right)^2 = \frac{f(n)}{\left(\frac{h_m}{d} \right)^2} \quad (5)$$

Equations (4) and (5) may also be written in the following form by canceling the bearing diameter d :

$$\frac{p}{\mu N'} \left(\frac{h_m}{l} \right)^2 = f(n) \quad (6)$$

$$\frac{p}{\mu N'} = \frac{f(n)}{\left(\frac{h_m}{l} \right)^2} \quad (7)$$

In this form the equations are limited to the range of values of l/d of less than 1 to which the short-bearing approximation specifically applies. As described in reference 6, if the equations are left in the form containing l/d as in equations (4) and (5), the range of applicability can be extended above $l/d = 1$ by the device of setting the $(d/l)^2$ term equal to 1 where l/d is greater than 1.

Analytical Curves From Short-Bearing Solution

The left-hand term of equation (5) which includes the bearing variable is the film capacity number and may be shown as a function of the film-thickness ratio h_m/d with eccentricity ratio as a parameter. For

constant values of n , equation (5) is hyperbolic in form as shown in figure 8. In figure 2, on logarithmic coordinates equation (5) gives a family of straight lines of slope equal to -2 , with the film capacity increasing as the film-thickness ratio h_m/d decreases.

In equation (2) it is to be noted that for any given value of h_m the value of n is determined by the bearing clearance c_d . Thus, in figure 3(a) the short-bearing-approximation lines are essentially a cross plot of figure 2, with the bearing clearance c_d substituted for n as a parameter.

The derivation of the curves of friction and peak-pressure ratio are shown in later sections.

Curves From Solutions of Cameron and Wood

In figures 2 and 3 analytical curves are also shown of load capacity and minimum film thickness based on the work of Cameron and Wood (ref. 7) whose solutions of Reynolds' equation are considered exact. The work of Cameron and Wood supplemented by that of Walther and Sassenfeld (ref. 12) gives values of eccentricity ratio and Sommerfeld numbers for l/d ratios from $1/8$ to 1.0 and for $l/d = \infty$. (The data given in ref. 12 extend the solution of Cameron and Wood and so credit is given to Cameron and Wood for these data in the figures.) As shown in figure 6, the Cameron and Wood curve for $l/d = 1.0$ agrees well with the average curve of the Cornell experimental data for values of l/d from $1/4$ to 1.0 when it is plotted in terms of load number $1/C_n$.

Cameron and Wood provide data based on eccentricity ratio and Sommerfeld number (n and S) which may be converted into data based on minimum film thickness by the following algebraic steps:

$$\frac{p}{\mu N'} \left(\frac{c_d}{d} \right)^2 = \frac{1}{S}$$

$$\frac{p}{\mu N'} \left(\frac{c_d}{d} \right)^2 \left(\frac{d}{l} \right)^2 = \left(\frac{1}{S} \right) \left(\frac{d}{l} \right)^2$$

Substituting for c_d from equation (2):

$$\frac{p}{\mu N'} \left(\frac{h_m}{d} \right)^2 \left(\frac{d}{l} \right)^2 = \left(\frac{1}{S} \right) \left(\frac{d}{l} \right)^2 \frac{(1-n)^2}{4} \quad (8)$$

$$\frac{p}{\mu N'} \left(\frac{d}{l}\right)^2 = \frac{\left(\frac{1}{S}\right) \left(\frac{d}{l}\right)^2 \frac{(1-n)^2}{4}}{\left(\frac{h_m}{d}\right)^2} \quad (9)$$

The family of Cameron and Wood curves in figure 2 may be obtained by substituting arbitrary values of n and corresponding values of S for a given value of l/d in the right-hand term of equation (9). The order of the lines labeled with values of n is nonlinear, with $n = 0.5$ giving greater film capacity numbers than either higher or lower values of n . Thus, the film capacity for a given film thickness will pass through a maximum at about $n = 0.5$. The value of n is dependent on the bearing clearance which is not shown in figure 2; that is, if values of h_m and n are assumed, the value of the bearing clearance c_d can be computed.

Effect of Varying Bearing Clearance

The analytical curves in figure 3(a) show the film capacity number against the ratio of bearing clearance to diameter with film thickness as a parameter. Figure 3(a) is essentially a cross plot of the analytical curves of figure 2 obtained by substituting the bearing-clearance ratio in place of the eccentricity ratio. This figure is one of the interesting results of this report. It also shows how the use of h_m facilitates the separation of the film thickness from the bearing clearance, in contrast with their combination in the eccentricity ratio.

The relationship of the three Cameron and Wood curves in each group shows the effect of changing the length-diameter ratio from 1 through $1/2$ to $1/4$. The relative location of the curves from the short-bearing solution in relation to the Cameron and Wood lines is of interest, and the extreme range of clearance change shown should be taken into consideration, since the clearance ratio is shown on a logarithmic scale.

In general, the Cameron and Wood curves in figure 3(a) show that the allowable load for a given minimum film thickness passes through a maximum at a small clearance and then decreases as the clearance ratio increases. They also show that bearings having very small l/d ratios are relatively less sensitive to large clearance ratio. A replot of portions of these curves on linear scales is enlightening, as shown in figure 3(b).

Unfortunately, the existing data in which eccentricity ratio or film thickness is measured are meager, and no adequate experimental data with sufficient range of bearing clearance could be found to permit

plotting experimental points in figure 3. However, some relevant comparisons are shown in figure 2 and subsequent figures.

Figure 9(a) shows curves of load number as given by equation (4) for the short-bearing approximation and equation (8) for the Cameron and Wood solution as well as values from the Sommerfeld solution. The product ph_m^2 in the load number appears on inspection to be indeterminate at $n = 1.0$, since the minimum film thickness h_m is zero and p becomes infinite in all solutions. For this reason these coordinates exaggerate the differences in the theories. This exaggeration is avoided by placing h_m^2 in the right-hand side of equation (5), as shown in figures 2 and 3.

The experimental data in figure 9(b) are also shown in figures 6 and 7 in which the experimental values of eccentricity ratio are plotted against the load number $1/C_n$. It may be seen that the deviations of the curves in figures 6 and 7 appear relatively small but that in figure 9 the deviations are greatly exaggerated.

EXPERIMENTAL DATA

Experimental data from four sources are shown for comparison with the analytical curves. Three of the sources of experimental data represent attempts to measure either eccentricity or minimum film thickness. The Cornell experimental data (refs. 5 and 6) and the data obtained on a different test machine by Kreisle (ref. 8) are based on measurements of eccentricity ratio which may be converted to minimum-film-thickness ratios. The experimental data by Dayton, Allen, Fawcett, Miller, and Grimble of the Battelle Memorial Institute (ref. 9) were obtained from direct measurements of minimum film thickness made by a method of voltage breakdown of the oil film as a dielectric. The fourth source of data is the work of Burwell, Kaye, Van Nymegen, and Morgan (ref. 10) who present experimental values of Sommerfeld numbers at the condition of a minimum coefficient of friction as a function of surface roughness of the bearing surfaces. Under this condition at the hook point, the surface roughness is shown to be related to the minimum oil-film thickness.

Cornell Experimental Data

Figure 6 shows the Cornell experimental data of eccentricity ratio against load number for bearings with values of l/d of $1/4$, $1/2$, and 1.0 in one group (ref. 5) and $1/4$ to 2 in another group (ref. 6).

Average curves for the two groups are shown in figure 6. The two average curves are nearly coincident except in the low-load region. In comparing these experimental curves with analytical curves, it may be seen that the Cameron and Wood curve of $l/d = 1.0$ is in better agreement with the experimental data than is the curve derived by the short-bearing approximation.

In the Cornell experiments, eccentricity measurements were made with dial gages through a mechanical linkage leading to a rubbing contact with the rotating shaft. Corrections were made for estimated changes in clearance at running conditions and the effect of shaft deflection on eccentricity measurements. Shaft speeds were from 500 to 7,000 rpm on a $1\frac{3}{8}$ -inch-diameter steel shaft and bronze bearings.

In figure 2, in which the Cornell experimental data are plotted to show film capacity number against minimum-film-thickness ratio, the Cornell data show agreement with the behavior predicted by the Cameron and Wood curves for $l/d = 1.0$ at various values of n . In figure 9(b) the Cornell data also agree well with the curves of Cameron and Wood although the differences are greatly magnified because of the nature of the plot.

It should be noted that for the Cornell data in which the l/d ratio is greater than 1 the $(d/l)^2$ terms in the load number, in the film capacity number, and in the abscissa of figure 9(b) are taken as unity. This device is employed in reference 6 since the experimental data show that bearing load capacity is essentially independent of l/d ratio for values of l/d from 1 to 2.

Kreisle's Experimental Data

Experimental eccentricity-ratio data as presented by Kreisle (ref. 8) are shown in figure 7 to show the effect of load number on eccentricity ratio. The test bearings used by Kreisle had l/d ratios from $1/53$ to $1/2$ and had a $1\frac{1}{8}$ -inch-diameter shaft. At $l/d = 1/53$, the bearing length is of sheet-metal thickness (0.021 inch), and the extreme shortness of the bearing accounts for the high load numbers obtained, since the $(d/l)^2$ term is approximately $(53)^2$ or 2,809.

As may be seen in figure 7, the curve from the short-bearing approximation agrees well with Kreisle's data. Figure 10 shows Kreisle's experimental point data plotted on coordinates of film capacity number against minimum-film-thickness ratio. The average curve through these data is shown among the summary curves of figure 2. As shown, the data cluster about the curves of the short-bearing approximation.

Kreisle's values of the film capacity numbers are high, reaching $162,000 \times 10^6$ for the bearing with $l/d = 1/53$, because of the $(d/l)^2$ term. In figure 11, the $(d/l)^2$ term is omitted from the film capacity number and a family of l/d curves is added as a parameter. Using $p/\mu N'$ as in figure 11, it may be seen that the film capacity number for all experimental data is less than 100×10^6 . A comparison of figures 10 and 11 shows the extent to which the $(d/l)^2$ term influences the magnitudes of the film capacity numbers.

The comparison between Kreisle's data and the short-bearing approximation is best shown in figure 7, where the differences of the experimental and analytical curves appear slight. The divergence in the range of load numbers from 10 to 100 is somewhat less than that of the Cornell experimental data. Values of l/d of $1/2$, $1/3$, and $1/5$ tend to predominate in this range because of the effect of the $(d/l)^2$ term.

The experimental curve for Kreisle's data shown in figure 9(b) is from the average curve through Kreisle's data plotted against load number in figure 7. In figure 9(b), discounting the exaggeration in this figure as previously explained, Kreisle's curve is in the shape of an S-curve crossing the analytical curve twice. The experimental data, in the region of n approaching 1, tend to show increasing values of $(p/\mu N')(h_m/d)^2(d/l)^2$ rather than a decline toward zero. This is interesting since the short-bearing approximation is the only theory giving an intercept other than zero.

Kreisle's data were obtained from coordinate measurements of eccentricity by using the movement of a core in a magnetic coil for an output signal. Through amplification, the signal was recorded to a high magnification. The test shaft was supported in a housing by two preloaded tapered-roller bearings with the test journal outboard of the roller bearings. The displacement under load of the nonrotating test bearing was measured relative to the housing. Considerable correction was necessary for the effect of shaft deflection on displacements and for the effect of temperature rise on bearing clearance.

Battelle Experimental Data

Dayton, Allen, et al. of Battelle Memorial Institute (ref. 9) appear to be the first experimenters to have measured minimum film thickness directly. In the words of the experimenters, "In these tests, a high audiofrequency voltage is applied across the oil film from a small electrode on the journal surface to the bearing. A cathode-ray oscillograph connected in parallel permits observation of the dielectric breakdown through the thin region of the oil film. The breakdown voltages are used to compute the thickness of the minimum oil film." Some

difficulties were experienced with movement of the electrode in the shaft with saw-tooth effects on the oscillograph picture.

In reference 9 the Battelle data are plotted as minimum film thicknesses in microinches against Sommerfeld number for a $1\frac{1}{4}$ - by $1\frac{1}{4}$ -inch bearing at speeds of 2,150, 3,550, and 4,950 rpm. Unit loads reached a value of 4,000 pounds per square inch using an SAE 10 oil. The data are summarized in a curve of eccentricity ratio against Sommerfeld number in which n ranges from 0.72 to 0.86. The curve from these data is shown in terms of load number $1/C_n$ in figure 6 for comparison with the analytical curves and with the Cornell experimental data. As may be seen, the Battelle data agree with the short-bearing approximation at the high load numbers, with some deviation at lower load numbers.

When plotted in terms of film capacity number and minimum-film-thickness ratio in figures 2 and 10, the Battelle data show good agreement with the short-bearing approximation. In the exaggerated form in figure 9(b) the experimental data again show a continuing increase in the abscissa as n approaches 1 rather than a decline toward zero as shown by the Cornell experimental data.

FILM THICKNESS AND SURFACE ROUGHNESS

In an investigation of the effect of surface finish on bearing friction, Burwell, Kaye, Van Nymegen, and Morgan (ref. 10) present values of Sommerfeld number at the point of minimum friction for various surface roughnesses. Figure 12 shows the nutcracker type of bearing test machine used by these investigators. As shown, the load is applied through two partial bearings against a common journal so that bending deformation of the shaft is not a variable in the experiments. The bearings used were $2\frac{1}{8}$ inches in diameter and 1.08 inches long

($l/d = 0.508$). SAE 30 oil was used, and the temperature of the oil film was measured by a thermocouple in the bottom bearing within $1/64$ inch from the bearing surface. The machine was equipped with apparatus to measure friction as shown.

Friction experiments were run to determine the Sommerfeld number at the hook point where the coefficient of friction reaches a minimum. In the region of hydrodynamic lubrication, the coefficient of friction declines as the load is increased, or as the Sommerfeld number is decreased, to a point where metallic contact of the peaks of the surfaces begins and an increase in friction coefficient becomes manifest. The experimental values of Sommerfeld numbers corresponding to points of minimum friction coefficient for bearings of various surface roughness

are given in table I. As shown, the measured surface roughnesses of the test journals varied from 130 microinches rms for turned surfaces to 1 microinch rms for superfinished surfaces. The surface roughnesses of the babbitted test bearings were estimated by the experimenters as 6 to 10 microinches rms. The experimental data in table I have been converted in terms of film capacity number and minimum-film-thickness ratio for comparison with the magnitude of the surface-roughness data.

When the peaks of the bearing and journal surfaces are at the beginning of contact, the minimum film thickness may be visualized as the sum of the surface-roughness values of the bearing and journal. However, a rigorous interpretation is required of the true magnitude of the surface roughness in terms of the root-mean-square values given by surface-analyzing instruments.

Tarasov (ref. 11) presents a clear picture of true surface roughness correlated with measurements by surface analyzers. The profiles of surfaces of hardened steel specimens finished by various processes were magnified 2,500 times in the vertical direction in order to determine what are termed by Tarasov as "deepest maximum" roughness and "predominant-peak" roughness. As shown in figure 13, the highest peaks and deepest valleys in the surface occur at relatively large intervals; the distance between a line drawn through these highest peaks and a parallel line through the deepest valleys is the deepest maximum roughness. A third line is drawn so that it intersects the valleys of the surface which occur at relatively frequent intervals. The distance between this line and the top line in figure 13 is the predominant-peak roughness and represents the roughness that occurs more or less uniformly over the whole surface. Both kinds of roughness are measured from the top line along which contact would first be made with an ideal mating surface.

The root-mean-square roughness values indicated by the analyzer are much smaller than the true roughnesses. Tarasov presents average values by which the root-mean-square value should be multiplied to determine the predominant-peak roughness of various types of finish for cylindrical surfaces. These values are: $4\frac{1}{2}$ for ground surfaces, $6\frac{1}{2}$ for hyperlapped, 7 for sandpapered, 7 for superfinished, and 10 for surfaces lapped by loose abrasives. Deepest maximum roughness is approximately twice the predominant-peak roughness.

Tarasov's magnifications of the irregularities of surfaces lead to a visualization of the profile of the thin fluid film of a heavily loaded journal bearing. Figure 14 shows an exaggerated view of the film profile for the condition at which the peaks of the bearing surface first made contact with the peaks of the journal surface. It is

at this condition that metallic friction begins to show the increase of bearing friction measured by Burwell et altera. The film thickness which exists at this condition may be idealized as if bounded by equivalent straight surfaces as shown in figure 14, and the thickness of the idealized film may be taken as the sum of the predominant-peak roughnesses of the two mating surfaces. Thus, the root-mean-square values of the two surface roughnesses given by Burwell et altera multiplied by the factors given by Tarasov may be added as an estimate of the magnitude of minimum film thickness at the condition prevalent at the hook point of friction curves.

Figure 4(a) shows film capacity number against minimum-film-thickness ratio reduced from the experimental data by Burwell et altera using Tarasov's correlation factors. As may be seen the data agree well with the analytical curve by the short-bearing solution. For comparison, the same data are shown in figure 4(b) in which minimum film thickness is evaluated from the root-mean-square values of surface roughness without Tarasov's factors. The calculations of $(p/\mu N')(d/l)^2$ and h_m/d from the data of reference 10 are shown in table I. An average value of 8 microinches rms is used for the surface roughness of the bearing surface in place of 6 to 10 microinches rms. Factors for ground and superfinished surfaces are available from Tarasov. For the turned surface, the factor of $4\frac{1}{2}$ for ground surfaces was used in the absence of the correct factor; and, similarly, in the absence of a correct factor for the grit-blasted surface the factor of 10 was used. The points corresponding to these estimates are those designated as noted in figure 4. Data for the etched surface are not included in figure 4 because of the lack of a correlation factor.

An important factor in the experiments by Burwell et altera is that care was taken to avoid running in the surfaces prior to the testing, since running in changes the surface roughness. It is also to be noted that the design of the bearing test machine was such that elastic deflection and misalignment of the journal and bearing were prevented.

FRICITION

Figure 5 gives analytical curves which indicate that the friction on the rotating journal and the power loss pass through a minimum as the bearing-clearance ratio varies. As shown for each l/d ratio and for each minimum film thickness, there is a clearance ratio for which the journal friction and power loss are a minimum, although for a range of clearance ratios near the optimum the change in journal friction is moderate. It is to be noted that the logarithmic scale of clearance

ratio shows very large changes. The bearing friction, however, that is, the friction on the stationary element, is shown to decrease as clearance ratio is increased and is a minimum at an infinite clearance ratio.

Mathematical Relationships

The curves of friction number against clearance ratio and minimum-film-thickness ratio of figure 5 are derived from the following mathematical analysis.

The short-bearing approximation (ref. 5) gives the following expression for friction force F without distinguishing between journal and bearing friction force because of the assumed linear velocity profile:

$$\begin{aligned} F &= 2\pi^2\mu N'ld \left(d/c_d \right) \frac{1}{(1-n^2)^{1/2}} \\ &= F_0 \frac{1}{(1-n^2)^{1/2}} \end{aligned} \quad (10)$$

in which $F_0 = 2\pi^2\mu N'ld \left(d/c_d \right)$ is the Petroff friction force.

In reference 6, it is shown that the friction force F agrees well with experimental measurements of the stationary-bearing friction as well as with the Cameron and Wood analytical curves for bearing friction. On this basis, equation (10) may be used to determine stationary-bearing friction force F_b . Thus

$$F = F_b = F_0 \frac{1}{(1-n^2)^{1/2}} \quad (11)$$

Reference 6 also indicates that journal friction force F_j is greater than F_b because of the couple formed by the applied load P and the lateral component of eccentricity e_h as shown in figure 1. In terms of friction torque, the couple T is:

$$\Delta T = \Delta F \frac{d}{2} = Pe_h = Pe \sin \phi \quad (12)$$

$$\Delta F \frac{d}{2} = Pe \sin \phi$$

$$\Delta F = Pe(\sin \phi) \frac{2}{d} \quad (13)$$

in which ΔF is friction force due to the couple, e is eccentricity, and ϕ is attitude angle. The variables P , e , and ϕ are functions of eccentricity ratio n . Substituting $P = \mu N' (d/c_d)^2 (l/d)^2 (1/C_n) ld$ and $e = n(c_d/2)$:

$$\Delta F = \mu N' (d/c_d) (l/d)^2 (1/C_n) ld n \sin \phi$$

$$\Delta F = F_o \frac{n(\sin \phi)(l/d)^2}{2\pi^2 C_n} \quad (14)$$

Journal friction force F_j is the sum of the bearing friction force and ΔF :

$$F_j = F_b + \Delta F$$

$$F_j = F_o \left[\frac{1}{(1-n^2)^{1/2}} + \frac{n(\sin \phi)(l/d)^2}{2\pi^2 C_n} \right] \quad (15)$$

In order to express equation (15) in terms of minimum film thickness, $(1-n)$ is introduced by algebraic manipulations as follows:

$$F_j = \frac{F_o}{(1-n)} \left[\frac{(1-n^2)^{1/2}}{(1+n)} + \frac{n(1-n)(\sin \phi)(l/d)^2}{2\pi^2 C_n} \right]$$

Substituting $F_o = 2\pi^2 \mu N' ld (d/c_d)$ and $(1-n) = 2h_m/c_d$:

$$F_j = \frac{\pi^2 \mu N' ld}{\left(\frac{h_m}{d}\right)} \left[\frac{(1-n^2)^{1/2}}{(1+n)} + \frac{n(1-n)(\sin \phi)(l/d)^2}{2\pi^2 C_n} \right]$$

$$\frac{(F_j/ld)}{\mu N'} \left(\frac{h_m}{d}\right) = \frac{\pi^2 (1-n^2)^{1/2}}{(1+n)} + \frac{n(1-n)(\sin \phi)(l/d)^2}{2C_n}$$

$$\frac{(F_j/ld)}{\mu N'} \left(\frac{h_m}{d} \right) = \psi(n) \quad (16)$$

The left-hand term of equation (16) groups the dimensional variables, including the minimum-film-thickness ratio (h_m/d), in nondimensional form. The function $\psi(n)$ is a function of eccentricity ratio except that the second term includes the l/d ratio as a parameter. Figure 15 shows the curves of equation (16) for l/d ratios of 1/2, 1, and 2. In order to determine the equation for the families of curves shown in figure 5 in terms of friction number, equation (16) may be rewritten:

$$\frac{(F_j/ld)}{\mu N'} = \frac{\psi(n)}{\left(\frac{h_m}{d} \right)} \quad (17)$$

In equation (17), for each assumed value of h_m/d , arbitrary values of clearance ratio give corresponding values of n and $\psi(n)$ such that the left-hand term, the friction number, may be plotted against clearance ratio with minimum-film-thickness ratio as a parameter.

In the friction number, the F_j/ld term may be regarded as unit friction loading in the same sense that unit loading is expressed as $p = P/ld$. Thus, the friction number is similar in form to $p/\mu N'$ and is dimensionless. The coefficient of friction f is the ratio of the two numbers.

The effect of l/d on the journal friction number is great as shown by comparing figures 5(a), 5(b), and 5(c). An inspection of equation (15) shows that at $l/d = 0$ the friction number is that for the bearing. The curves for bearing friction are shown in figure 5 for comparison with the curves for journal friction. The increasing differences of the two frictions as l/d is increased are shown also in figure 15. The curves show friction force per unit area in dimensionless form, which is proportional to friction torque and power loss for a given diameter.

The curves of figure 15 show in one chart the effect of l/d ratio and eccentricity ratio on the friction number when h_m/d is regarded as constant. The curves also show that the minimum value of the journal friction number is at some value of n ranging from $n = 0.25$ for $l/d = 2$ to about $n = 0.9$ for $l/d = 1/2$.

PEAK-PRESSURE RATIO

The ratio of the peak or maximum local pressure p_{\max} in the fluid film to the unit bearing load p on a projected area is called the peak-pressure ratio. For heavily loaded bearings supported on extremely thin films, p_{\max} may be many times the unit load p and may cause yielding or fatigue of the bearing material.

In reference 5, the peak-pressure ratio k is shown to be a function of eccentricity ratio as given in the following equations from the short-bearing approximation in which θ_{\max} gives the angular location of p_{\max} :

$$k = \frac{p_{\max}}{p} = C_n \frac{6\pi n \sin \theta_{\max}}{(1 + n \cos \theta_{\max})^3} \quad (18)$$

$$\theta_{\max} = \cos^{-1} \left[\frac{1}{4n} \left(1 - \sqrt{1 + 24n^2} \right) \right] \quad (19)$$

The short-bearing-approximation lines in figure 3 showing film capacity number against clearance ratio are repeated in figure 16 to show how the eccentricity ratio is involved as a parameter. The lines of constant n shown are also lines of constant peak-pressure ratio k . It may be seen that for very thin films and for large clearances the eccentricity ratio and peak-pressure ratio become great. At $n = 0.99$, the peak pressure is 22 times the unit load. In figure 17, peak-pressure ratio is shown plotted against clearance ratio with minimum-film-thickness ratio as a parameter, and eccentricity ratio is eliminated as a variable. It can be seen from these figures that the peak-pressure ratio in the oil film rises rapidly with eccentricity ratio and with increasing bearing clearance.

ANALYSIS AND DISCUSSION

As may be seen in figures 3, 4(a), and 5(b), for example, the use of the minimum thickness of the oil film as a basic variable has been fruitful, not only for its ability to illustrate the effects of film thickness and bearing clearance separately but also for its ability to lead to a more penetrating understanding of bearing performance. Each of these types of curves invites discussion to suggest reasons for the performance indicated.

It is to be noted that the short-bearing approximation has been used in this report chiefly as a vehicle for obtaining types of curves on which exact analytical solutions and experimental data could be plotted. The equation form of the short-bearing approximation facilitates the plotting of a first approximate curve which then requires other data to be plotted in a similar manner for comparison.

This view of the short-bearing approximation may be unnecessarily severe, since all of the analytical solutions shown are based on the simplifying assumption of constant viscosity and temperature of the oil film as it moves around the journal. The general agreement of the experimental data with the analytical curves shown seems to justify this assumption, but the assumption offers an explanation of the difference between the so-called exact analytical curves and the experimental data.

The effect of high local pressures in the thin region of the oil film increases the viscosity of the oil considerably, although this effect is counteracted to an unknown extent by the increase in temperature of the oil film in the same areas, which tends to reduce the viscosity. If the pressure-viscosity effect exceeds the temperature-viscosity effect, an increase in local viscosity of the oil film would tend to increase the experimental values of film thickness over that shown by the exact analytical curves, and the effect would increase at high values of eccentricity and peak pressure in the oil film.

In figure 2, which summarizes the data for load against film thickness in this report, the experimental data of Kreisle, Burwell, et alera and Battelle all tend to show somewhat larger film thickness than the exact analytical solutions of Cameron and Wood and are in closer agreement with the short-bearing-approximation curves. Thus, the omission of one of the leakage terms in the short-bearing approximation tends to increase the predicted film thickness and the effect as shown by figure 2 may be toward closer agreement with experimental data taken under severe conditions. However, in view of the difficulty of measuring film thickness with sufficient accuracy, the effects of these counteracting errors are conjectural rather than conclusive.

It is recommended that experimental curves of eccentricity ratio and film thickness be used when available, since the analytical curves of the short-bearing approximation show a larger film thickness than do the experimental data in the moderate-load range of load numbers from 10 to 200. At higher load numbers the short-bearing analytical curves are in closer agreement with the available experimental data.

Effect of Bearing Clearance on Load Capacity

In figure 3(a) it is evident that the divergence of the short-bearing approximation from the exact solution increases as the bearing clearance increases. This indication should be considered in the light of the assumption adopted in making the short-bearing approximation, namely, that all of the leakage flow in the converging film is included, except that part of the circumferential flow related to the pressure differential in the circumferential direction.

If a journal bearing having a relatively large clearance is considered, the angular extent of the effective portion of the oil film is confined to a small angle near the load line. In this situation, the rate of change of pressure in the circumferential direction designated dp/dx becomes large because the pressure drop must occur in a short distance. Thus the leakage flow in the circumferential direction becomes relatively larger as the clearance-diameter ratio increases. This is the leakage term which is neglected in the short-bearing approximation in order to obtain an integration in the form of an equation.

This reasoning seems to indicate that in addition to the limitation of the short-bearing approximation in regard to l/d , a second limitation in regard to c_d/d is advisable. Thus for large clearance-diameter ratios, the short-bearing approximation apparently applied to a smaller range of l/d ratios than it does at small clearance ratios. This added limitation explains the effects indicated by the hundredfold increase in clearance ratio shown on figure 3, where the relation of the short-bearing approximation to the exact lines of Cameron and Wood indicates that it applies to bearings with very small l/d ratios at large values of c_d/d .

Correlation of Predicted Film Thickness With Surface Roughness

The correlation of the film thickness predicted at the hook point of friction curves with the predominant-peak roughness values obtained from Tarasov's conversion factors as shown in figure 4(a) illustrates the value of the use of h_m as a basic variable. The curve was first obtained in the form shown in figure 4(b), where an error of four to one or more is apparent when root-mean-square roughness values are used. Tarasov's paper, which gave the proper interpretation of root-mean-square values, supplied the answer nicely.

If the comparison of figure 4(a) were made with a Cameron and Wood line for $l/d = 1/2$, the analytical line would lie slightly to the left

of the experimental points, being part way to the lines shown for $l/d = 1$ in figure 2. This might be explainable on the basis that while the experimenters made an effort to avoid running in the bearing, a partial wearing off of the peaks of the roughness had already occurred by the time the data could be taken so that the film thickness at touching was less than that indicated by the predominant-peak roughness.

In order to obtain similar results in ordinary bearings in service two factors present in the bearing test machine shown in figure 12 must be satisfied. These factors are: (1) Perfect alinement of the bearing with the journal by central application of the load, and (2) absence of elastic deflection of the shaft which would deform the journal in an elastic curve. The elastic curvature of the journal in a steady state can often be accommodated by the conformability of soft bearing materials, but it is unfortunately true that the height of the elastic curve within the length of a bearing is generally large when compared with the minimum thickness of the oil film.

Figure 4(a) illustrates a method of correlation of the minimum obtainable film thickness under conditions of perfect alinement with analytical values of film thickness and thus closes the missing link needed to permit prediction of the load number, in figure 6, for example, at which failure conditions are apt to originate. If elastic curvature of the shaft is also present, an allowance for the height of the elastic curve within the bearing length should be added as indicated in reference 5. While the basic procedure is now on a firm footing, the details of how to allow for running in of soft bearing surfaces become an interesting point for further investigation.

Effect of Clearance on Friction and Power Loss

Figure 5 indicates an increase of friction torque on the rotating element or journal as the bearing clearance is increased. Since it is the friction on the rotating element which is related to power loss, this increase is important, but a more reasonable idea of the magnitude of the increase is obtainable from the curves by assuming a reasonable increase of clearance ratio, thus avoiding the hundredfold increase in clearance possible on the logarithmic scales. The logarithmic vertical scale, on the other hand, tends to hide some of the increase, so that a plot of values on linear scales is advisable for any particular application.

For the range of diametral-clearance ratio from 0.001 to 0.005, the actual change in journal friction depends on the proximity of the minimum point on the friction curve, which depends on l/d ratio as shown in figure 5. For $l/d = 1/2$, the effect of a limited increase

in clearance is a small reduction of power loss except at high loads; at $l/d = 1$, the effect is small at light loads, becoming a moderate increase in friction at high loads; while at $l/d = 2$, an increase of clearance causes a general rise in power loss.

The explanation of the increase of power loss with increasing clearance is a simple extension of the material contained in an earlier report (ref. 6). This material indicated that an improved correlation of friction torque on the rotating element is obtained by adding the couple produced by the load line acting at a small lateral displacement from the center of the bearing. This displacement is shown in figure 1 as e_h which is equal to the eccentric displacement e times the sine of the attitude angle. It can be shown analytically that the friction on the bearing and the journal differ by the amount of this couple. Thus, if the bearing clearance is increased, the eccentricity e is increased, resulting in an increase in the load couple and in the friction torque on the rotating element. This effect is balanced somewhat by the decrease in viscous friction, so that the curves pass through a minimum as shown.

The addition of the load couple described above is to be used with the method of estimating friction described in reference 6, in which the friction of the stationary element is obtained by multiplying the Petroff friction at no load by the friction ratio to obtain the friction of the stationary element under load. The friction of the rotating element is then obtained by adding the load couple.

This method of estimating the friction of full journal bearings avoids the use of the troublesome concept of a coefficient of friction and obtains the result directly from fundamental principles. It is hoped that a wider use of these methods will allow closer estimates of power loss to be obtained reliably.

CONCLUSIONS

The following conclusions may be drawn from the results of this investigation on the relation of journal bearing performance to minimum oil film thickness:

1. The effects of changes in film thickness and in bearing clearance on load capacity, friction, and peak-pressure ratio may be shown separately by the use of the minimum thickness of the oil film as a basic variable.

2. The major control of load capacity lies in the minimum film thickness; the effects of changes in clearance diminish with small length-diameter ratios.

3. In general, the load capacity passes through a maximum at a small bearing clearance and then decreases with increasing bearing clearance, the effect diminishing with decreasing length-diameter ratio, so that very short bearings are less sensitive to increasing bearing clearance.

4. The friction torque on the rotating element and the power loss pass through a minimum and then rise with increasing clearance because of the effect of the couple produced by the load and the lateral displacement.

5. The peak-pressure ratio in the oil film rises rapidly with eccentricity ratio and with increasing bearing clearance.

6. The range in which the analytical curves of the short-bearing approximation are acceptable is limited by increases in bearing clearance as well as in length-to-diameter ratio.

7. It is recommended that experimental curves of eccentricity ratio and film thickness be used when available, since the analytical curves of the short-bearing approximation show a larger film thickness than do the experimental data in the moderate-load range of load numbers from 10 to 200. At higher load numbers the short-bearing analytical curves are in closer agreement with the available experimental data.

Cornell University,
Ithaca, N. Y., March 14, 1956.

REFERENCES

1. Dennison, E. S.: Film-Lubrication Theory and Engine Bearing Design. Trans. A.S.M.E., vol. 58, no. 1, Jan. 1936, pp. 25-36.
2. Boyd, J., and Raimondi, A. A.: Applying Bearing Theory to the Analysis and Design of Journal Bearings. Paper no. 53, Design Data and Methods, A.S.M.E., 1953, pp. 123-141.
3. Kingsbury, A.: Optimum Conditions in Journal Bearings. Trans. A.S.M.E., RP-54-7, vol. 54, 1932, pp. 123-148.
4. Needs, S. J.: Effects of Side Leakage in 120° Centrally Supported Journal Bearings. Trans. A.S.M.E., APM-56-16, vol. 56, 1934, pp. 721-732.
5. DuBois, George B., and Ocvirk, Fred W.: Analytical Derivation and Experimental Evaluation of Short-Bearing Approximation for Full Journal Bearings. NACA Rep. 1157, 1953.
6. DuBois, G. B., Ocvirk, F. W., and Wehe, R. L.: Experimental Investigation of Eccentricity Ratio, Friction, and Oil Flow of Long and Short Journal Bearings with Load-Number Charts. NACA TN 3491, 1955.
7. Cameron, A., and Wood, W. L.: The Full Journal Bearing. Proc. Institution Mech. Eng. (London), vol. 161, W.E.P. Nos. 47-54, 1949, pp. 59-72.
8. Kreisler, L. F.: Very Short Journal-Bearing Hydrodynamic Performance Under Conditions Approaching Marginal Lubrication. Trans. A.S.M.E., vol. 78, no. 5, July 1956, pp. 955-963.
9. Dayton, R. W., Allen, C. M., Fawcett, S. L., Miller, N. E., and Grimble, R. E.: A Fundamental Study of Bearing Behavior. Contract N5 ori-111, Office Naval Res. and Battelle Memorial Inst., May 16, 1952.
10. Burwell, J. T., Kaye, J., Van Nymegen, D. W., and Morgan, D. A.: Effects of Surface Finish. Jour. Appl. Mech., vol. 8, no. 2, June 1941, pp. A-49-A-58.
11. Tarasov, L. P.: Relation of Surface-Roughness Readings to Actual Surface Profile. Trans. A.S.M.E., vol. 67, no. 3, Apr. 1945, pp. 189-196.

12. Walther, A., and Sassenfeld, H.: Druckverteilung und Last im 360° - Gleitlager im Bereich der Gedrunge - heiten (Verhältnis von Durchmesser zur Länge) $B = 0$ bis $B = 8$ für die Eccentrizitäten $c = 0.1$ bis $c = .95$. Ber. 8, Inst. für praktische Math., Tech. H. S. Darmstadt, 1950. (Available in translation as: Pressure Distribution and Load in a 360° Journal Bearing, for Values of the Characteristic B (Ratio of Diameter to Length) from 0 to 8, and Eccentricities $C = 0.1$ to $C = 0.95$. Rep. no. 11, Sponsored Res. (Germany), Dept. Sci. and Ind. Res. (Gr. Brit.), 1950.

TABLE I

DETERMINATION OF MINIMUM FILM THICKNESS AND LOAD CAPACITY AT POINT OF MINIMUM
FRICTION FROM EXPERIMENTAL DATA OF REFERENCE 10

[Minimum-film-thickness determinations are based on measured root-mean-square values of surface roughness corrected by Tarasov's factors giving surface roughness in terms of predominant-peak roughness (see figs. 4, 13, and 14);
 $l = 1.08$ in., $d = 2\frac{1}{8}$ in.]

Type of finish (a)	Surface roughness, μ n. rms				Factor given by Tarasov (ref. 11)	Minimum film thickness, h_m in.	Minimum-film-thickness ratio, h_m/d	d/c_d (a)	Sommerfeld no. at point of min. friction, S (a)	Film capacity number, $\frac{p}{\mu N'} \left(\frac{d}{l}\right)^2$ (c)
	Journal		Bearing (b)	Sum of maximum journal and bearing						
	Transverse (a)	Parallel (a)								
Turned	130	50	8	138	$d \frac{1}{2}$	620×10^{-6}	291×10^{-6}	1,150	0.38	13.5×10^6
Ground	70	70	8	78	$\frac{1}{2}$	351	165	1,200	.25	22.4
Ground	50	50	8	58	$\frac{1}{2}$	261	125	650	.06	25.7
Grit-blasted	30-50	--	8	48	$\frac{1}{10}$	480	226	280	.12	2.54
Ground	14	--	8	22	$\frac{1}{2}$	99	46.5	520	.0017	616
Ground	13	--	8	21	$\frac{1}{2}$	94.5	44.5	540	.0013	870
Chemically etched	11	--	8	19	(f)	-----	-----	280	.024	12.7
Ground	7	8	8	16	$\frac{1}{2}$	72	33.8	500	.0012	808
Ground	4	6	8	14	$\frac{1}{2}$	63	29.6	480	.001	894
Superfinished	1	--	8	9	7	63	29.6	500	.0008 to .0011	1,212 to 881

^aData from ref. 10.

^bBabbitt bearing surface roughness was stated as 6 to 10 μ n. rms.

^c $(p/\mu N')(d/l)^2 = (1/S)(d/c_d)^2(d/l)^2$ where $l = 1.08$ in. and $d = 2\frac{1}{8}$ in.

^dFactor for ground surfaces used in absence of correct factor.

^eFactor for loose-abrasive lapped surfaces used in absence of correct factor.

^fFactor not given.

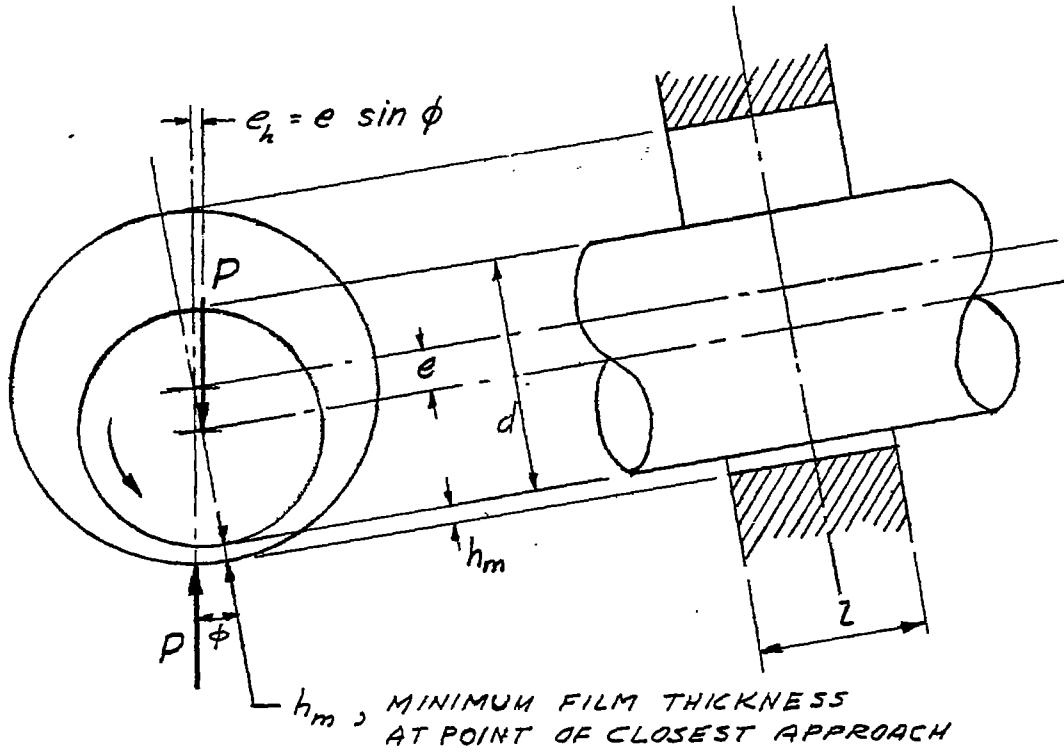


Figure 1.- Journal bearing with steady central load.

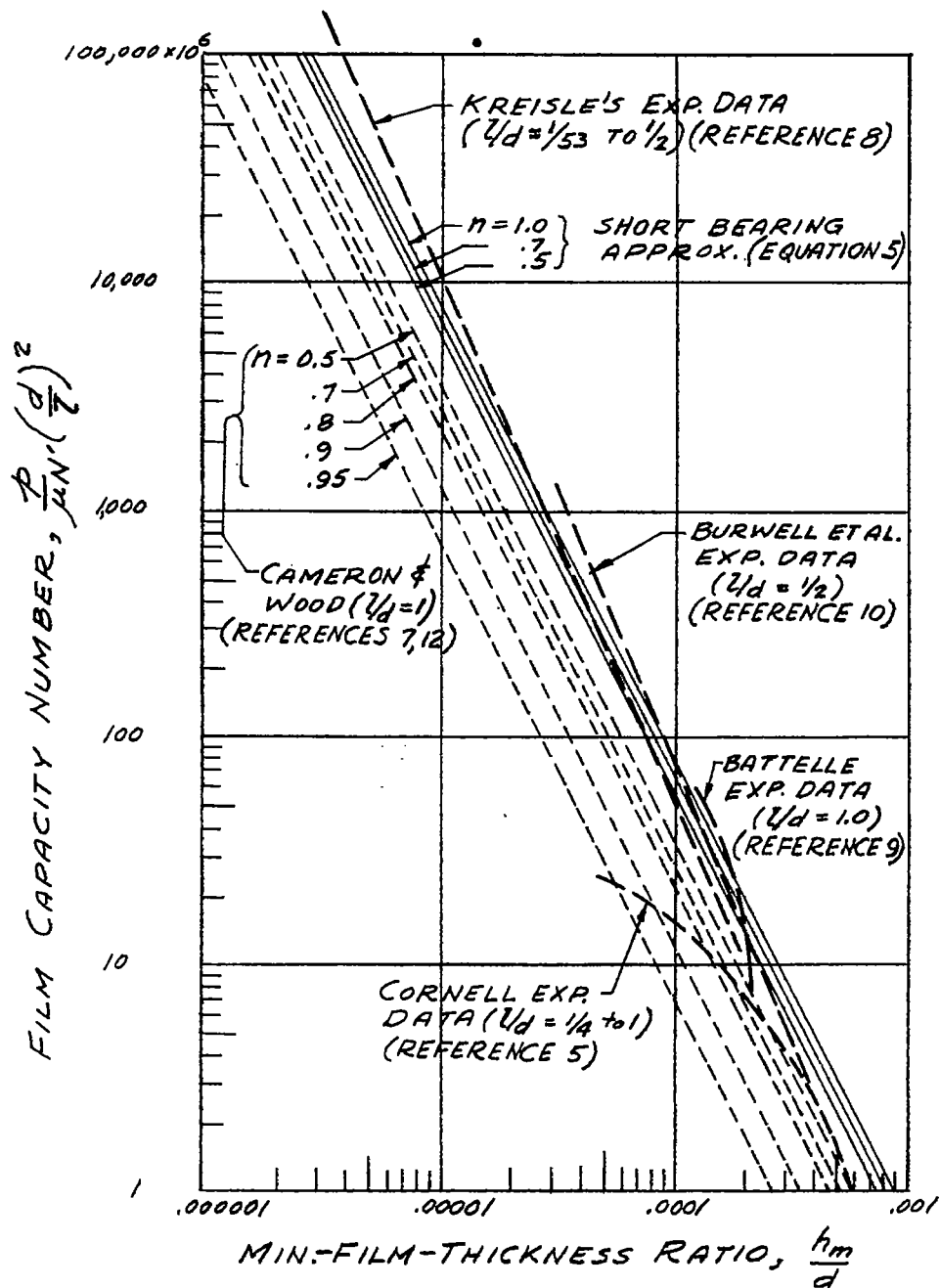
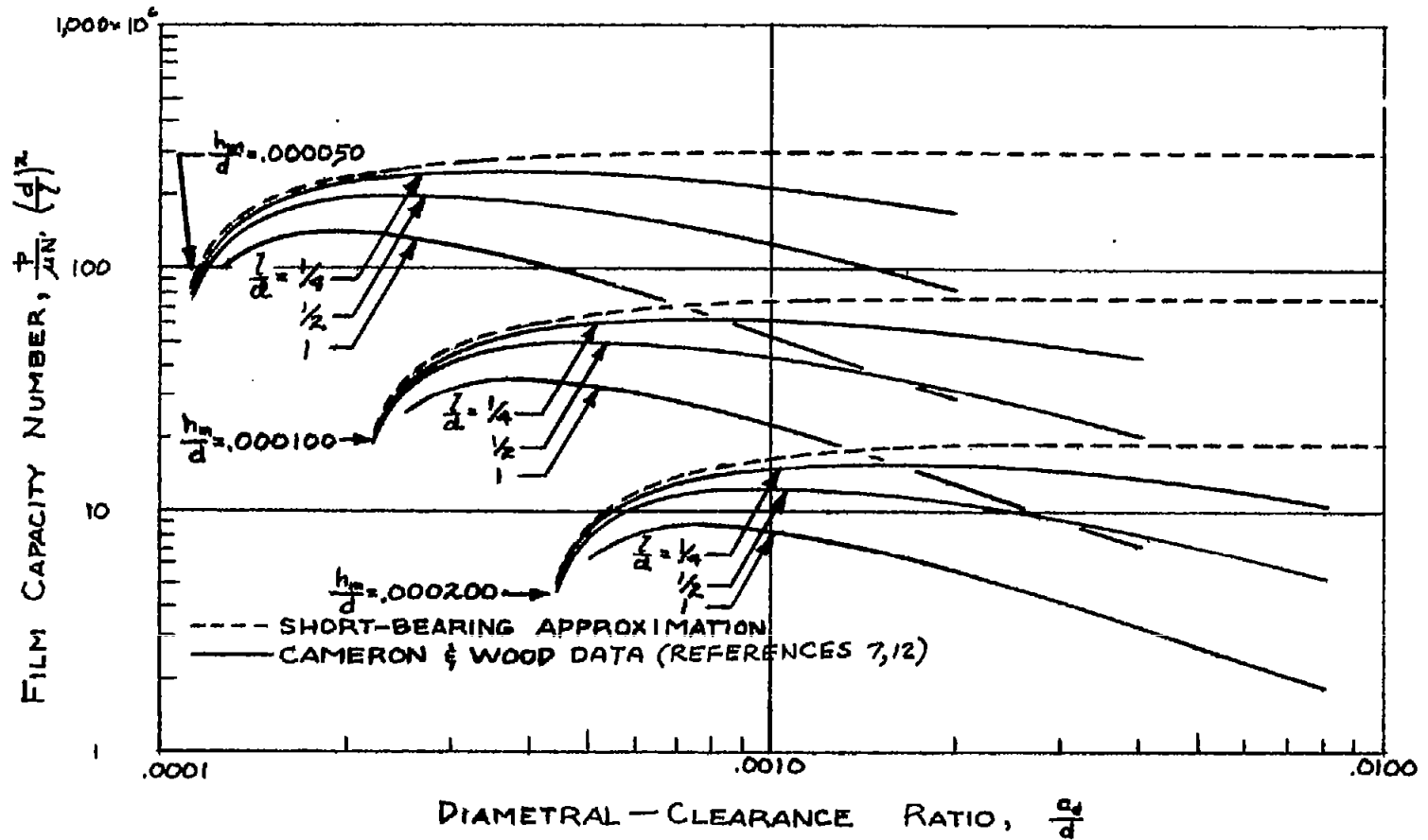
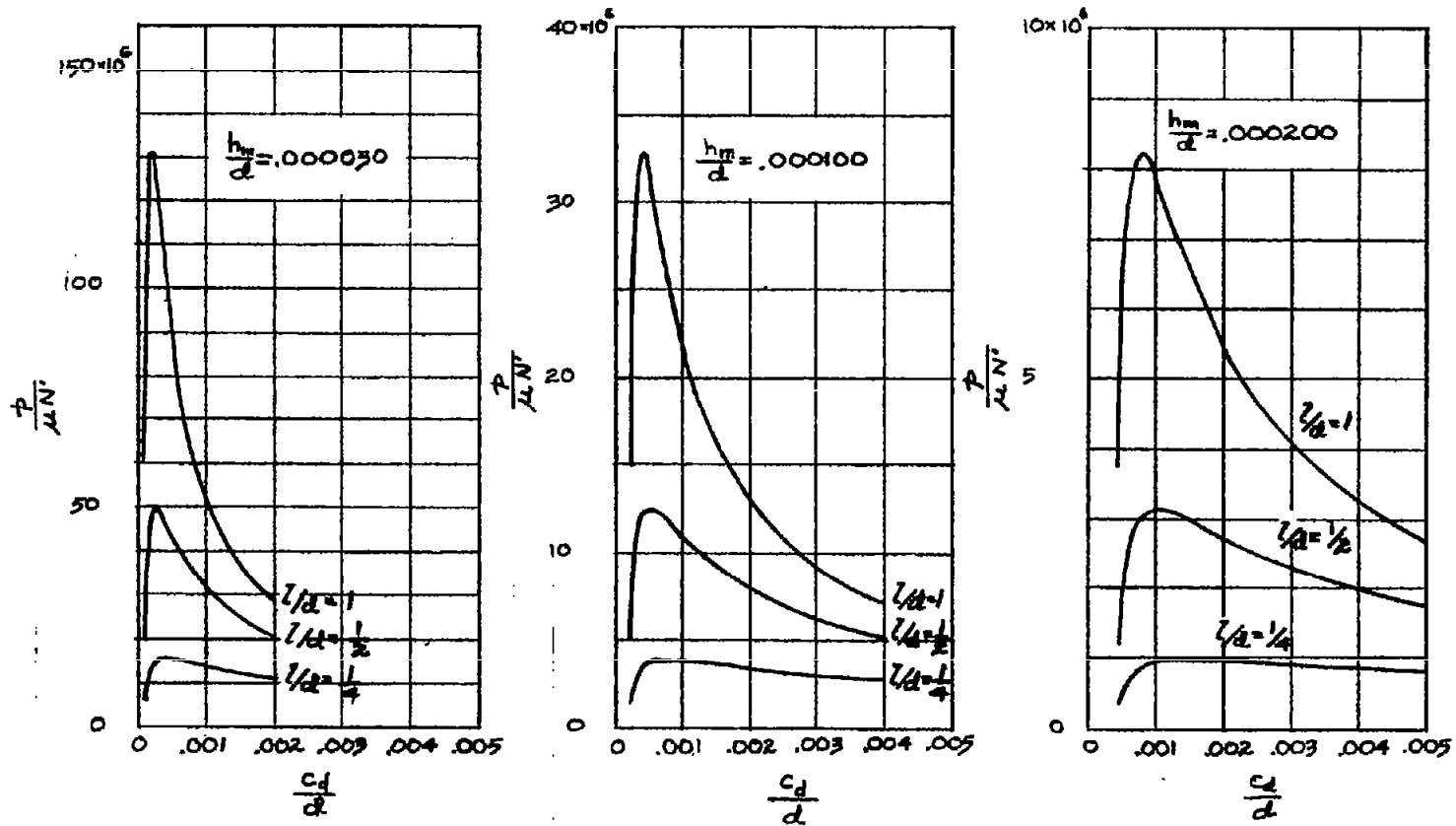


Figure 2.- Curves showing relationship of bearing load capacity and minimum film thickness in nondimensional form. Experimental curves from four sources are compared with two analytical solutions. In ordinate scale, for $l/d > 1.0$ use $d/l = 1.0$.



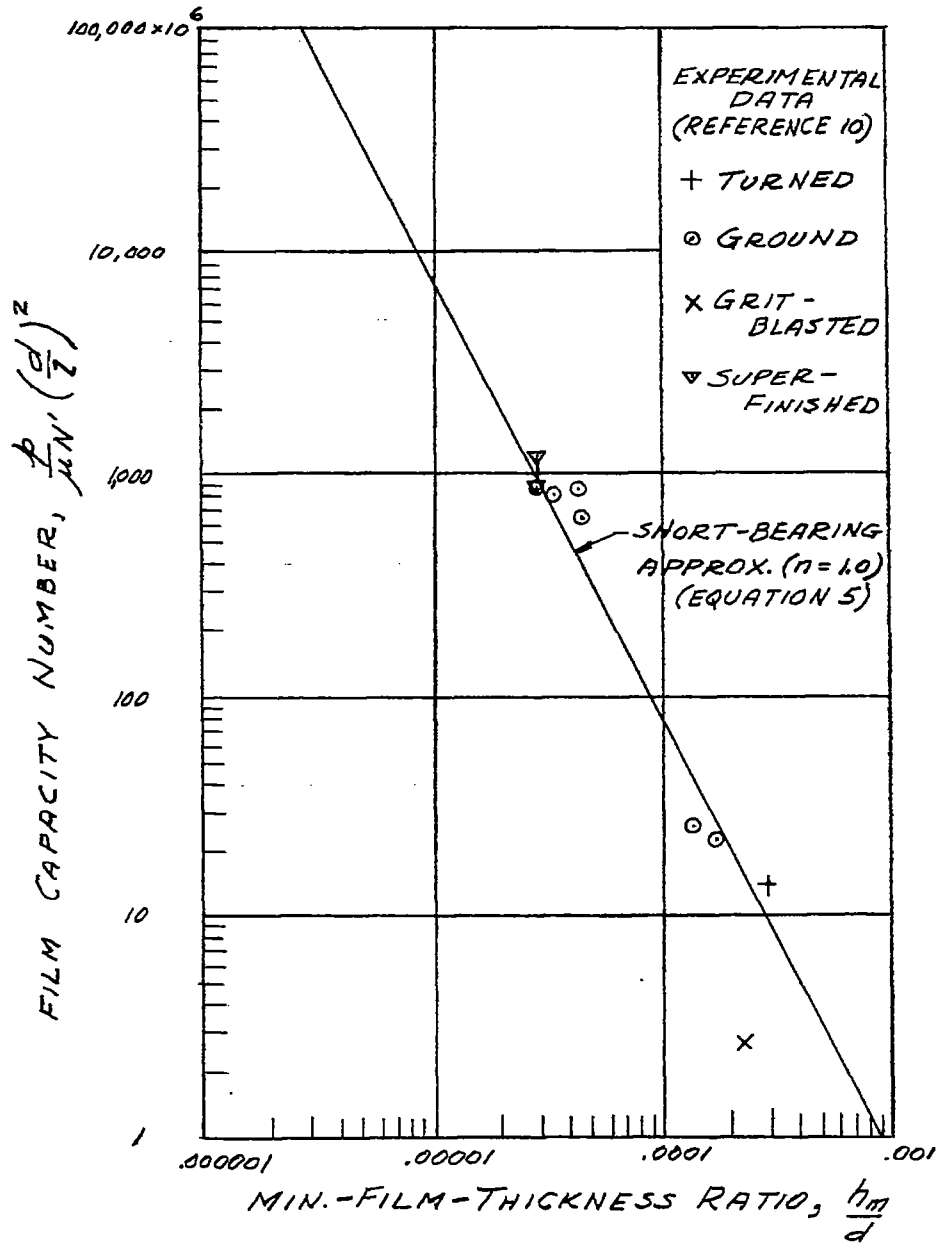
(a) Curves plotted on logarithmic scales. In ordinate scale, for $l/d > 1.0$ use $d/l = 1.0$.

Figure 3.- Analytical curves showing effect of bearing-clearance changes on bearing load capacity at various ratios of minimum oil-film thickness.



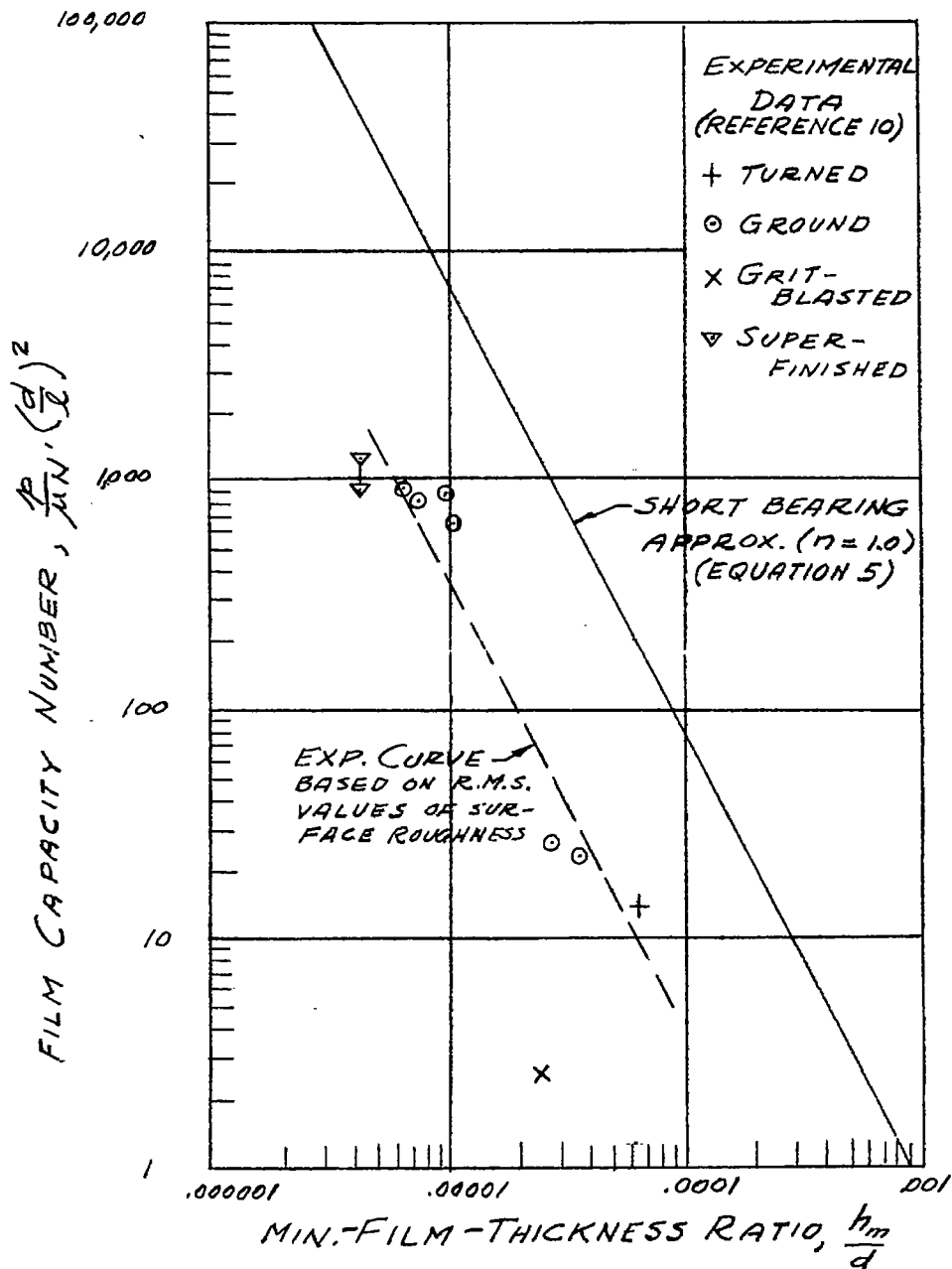
(b) Curves plotted from data of Cameron and Wood (refs. 7 and 12) on linear scales.

Figure 3.- Concluded.



(a) Data points show minimum film thicknesses as determined from measured surface roughnesses corrected by Tarasov's factors (ref. 11).

Figure 4.- Comparison of curve of short-bearing approximation (eq. (5)) with experimental data of Burwell, Kaye, Van Nymegen, and Morgan (ref. 10). $l/d = 1/2$.



(b) Minimum film thicknesses determined from root-mean-square values of surface roughnesses without using Tarasov's factors.

Figure 4.- Concluded.

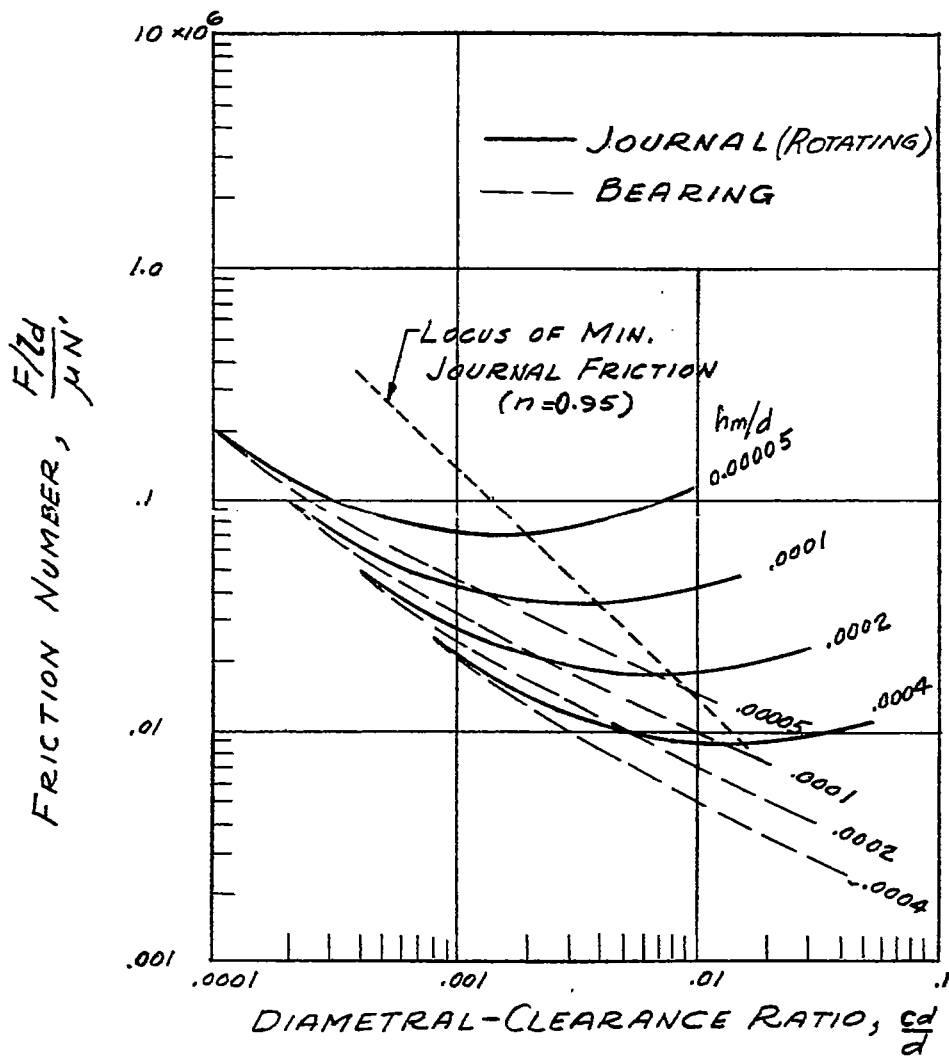
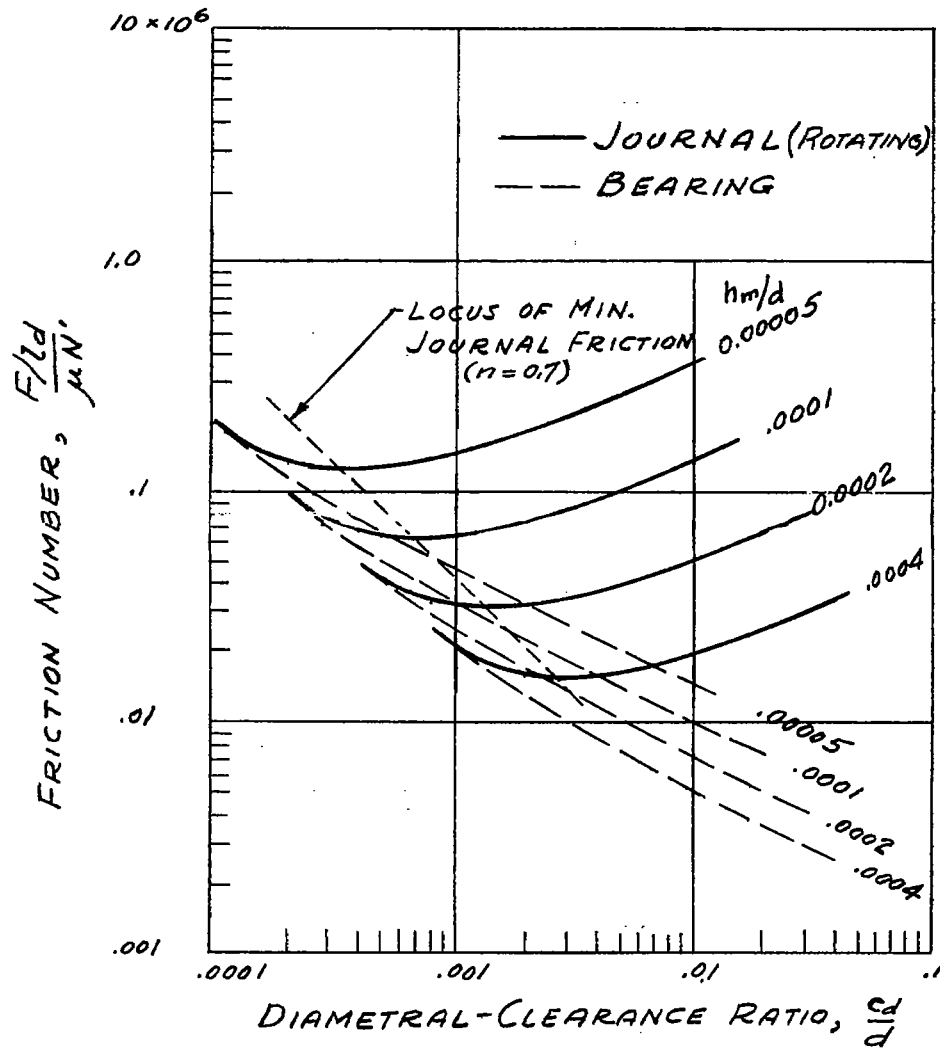
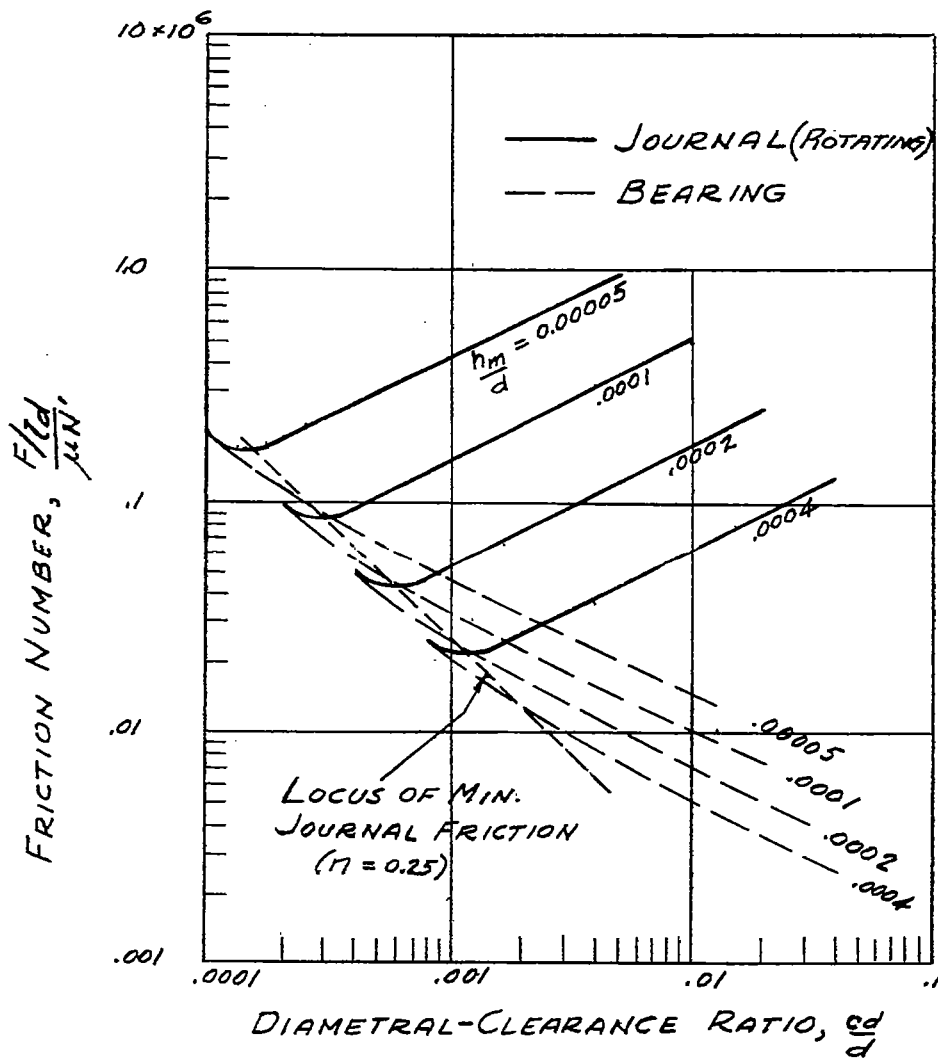
(a) $l/d = 1/2$.

Figure 5.- Influence of bearing clearance and minimum film thickness on journal and bearing friction as shown by analytical curves from short-bearing approximation (see eq. (17)). Clearance for minimum journal friction decreases with increasing values of l/d ; effect of load couple on friction of rotating element increases with increasing values of l/d .



(b) $z/d = 1.$

Figure 5.- Continued.



(c) $l/d = 2$.

Figure 5.- Concluded.

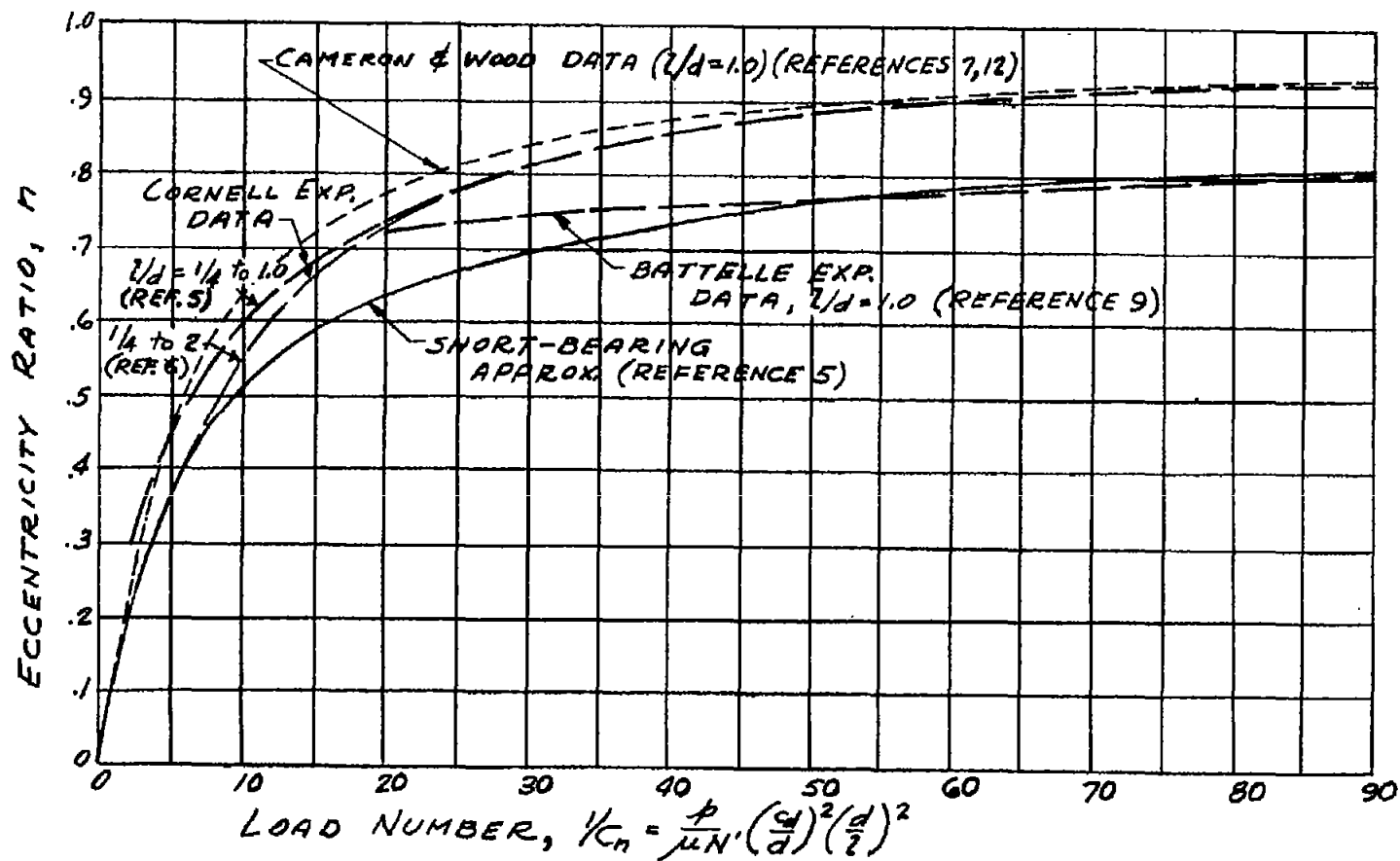


Figure 6.- Comparison of two analytical curves with curves from experimental data showing effect of load number on eccentricity ratio. In abscissa scale, for $l/d > 1.0$ use $d/l = 1.0$.

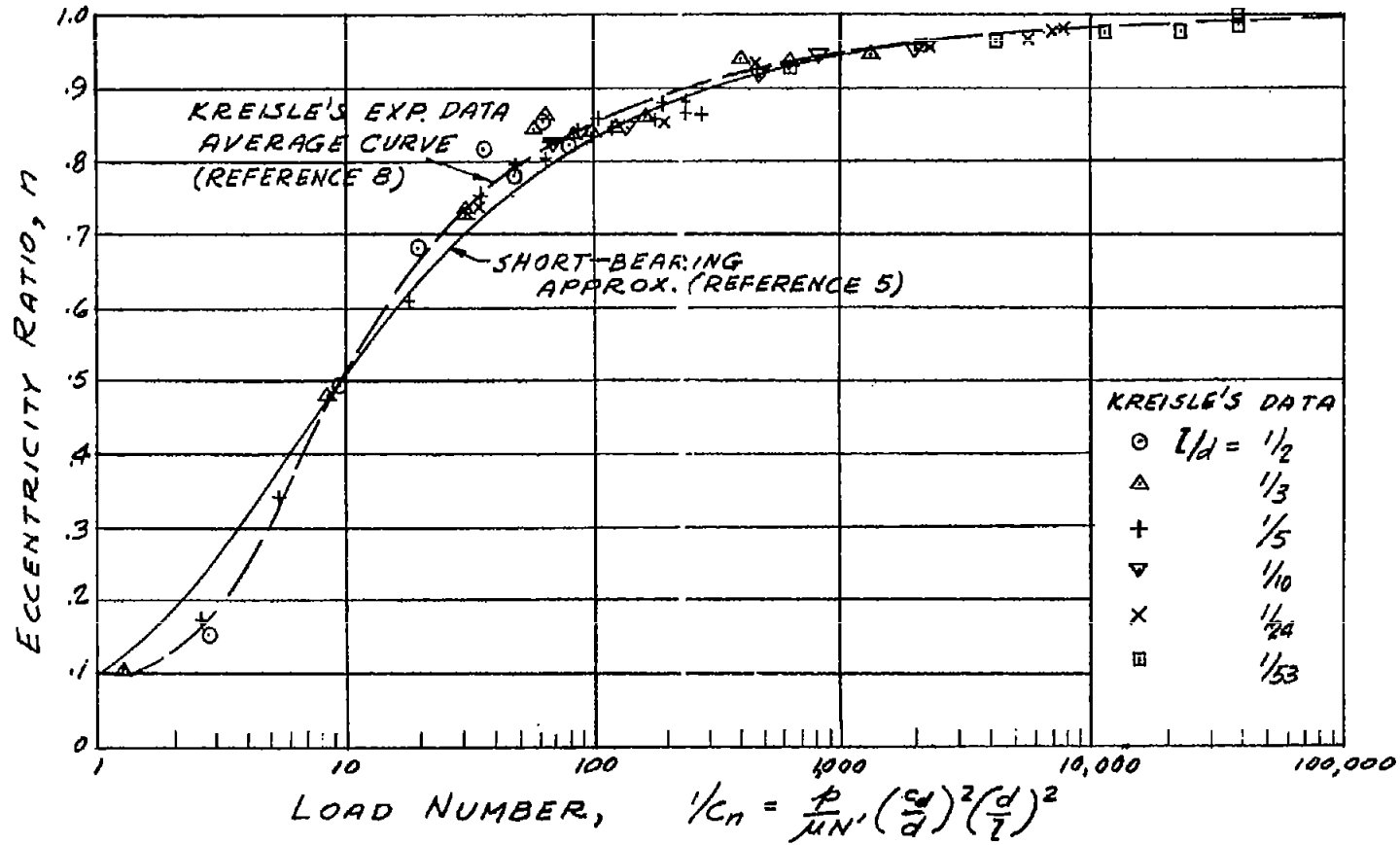


Figure 7.- Comparison of eccentricity ratio of very short bearings with analytical curve of short-bearing approximation using experimental data from Kreisle (ref. 8) for l/d ratios from $1/2$ to $1/53$.

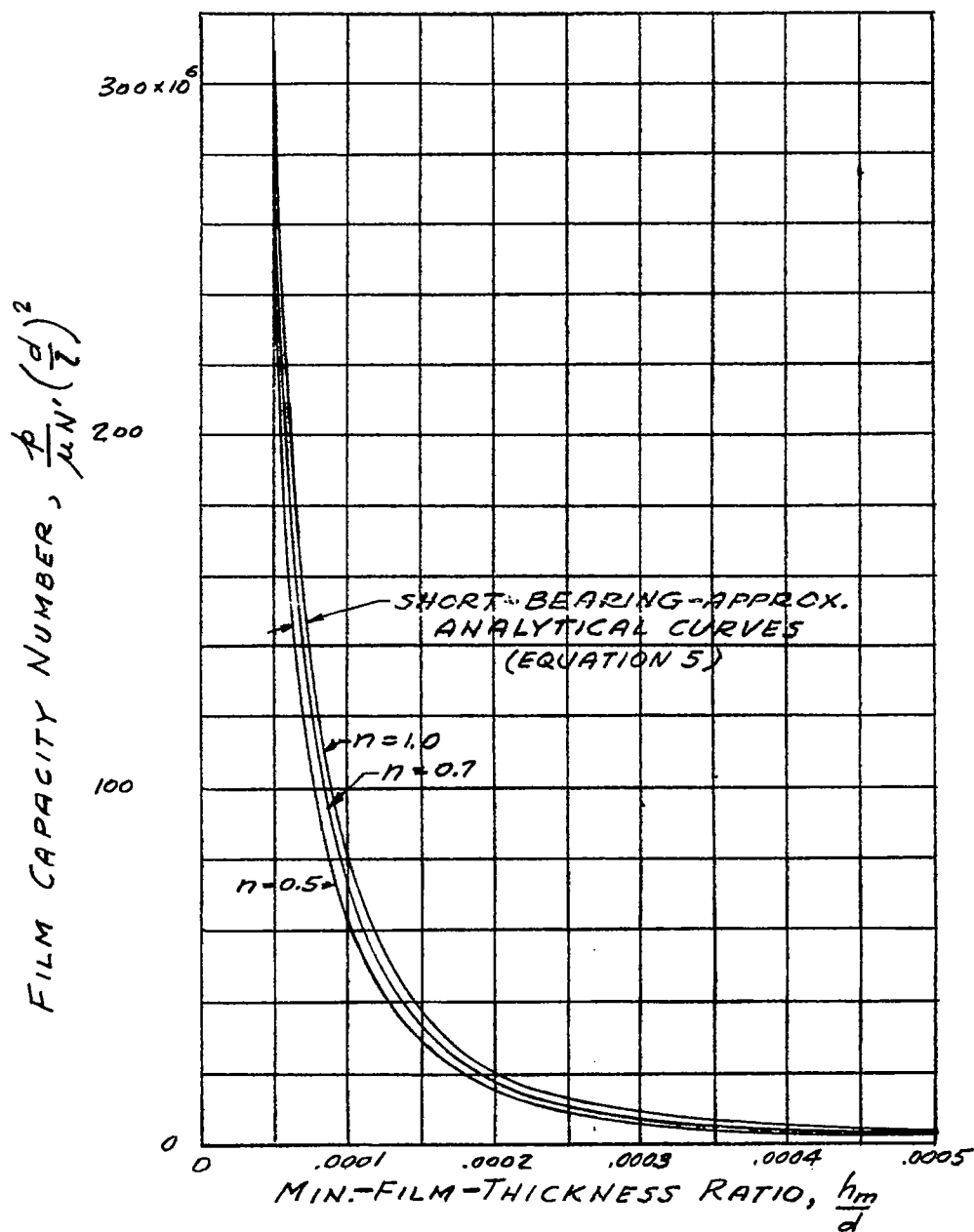
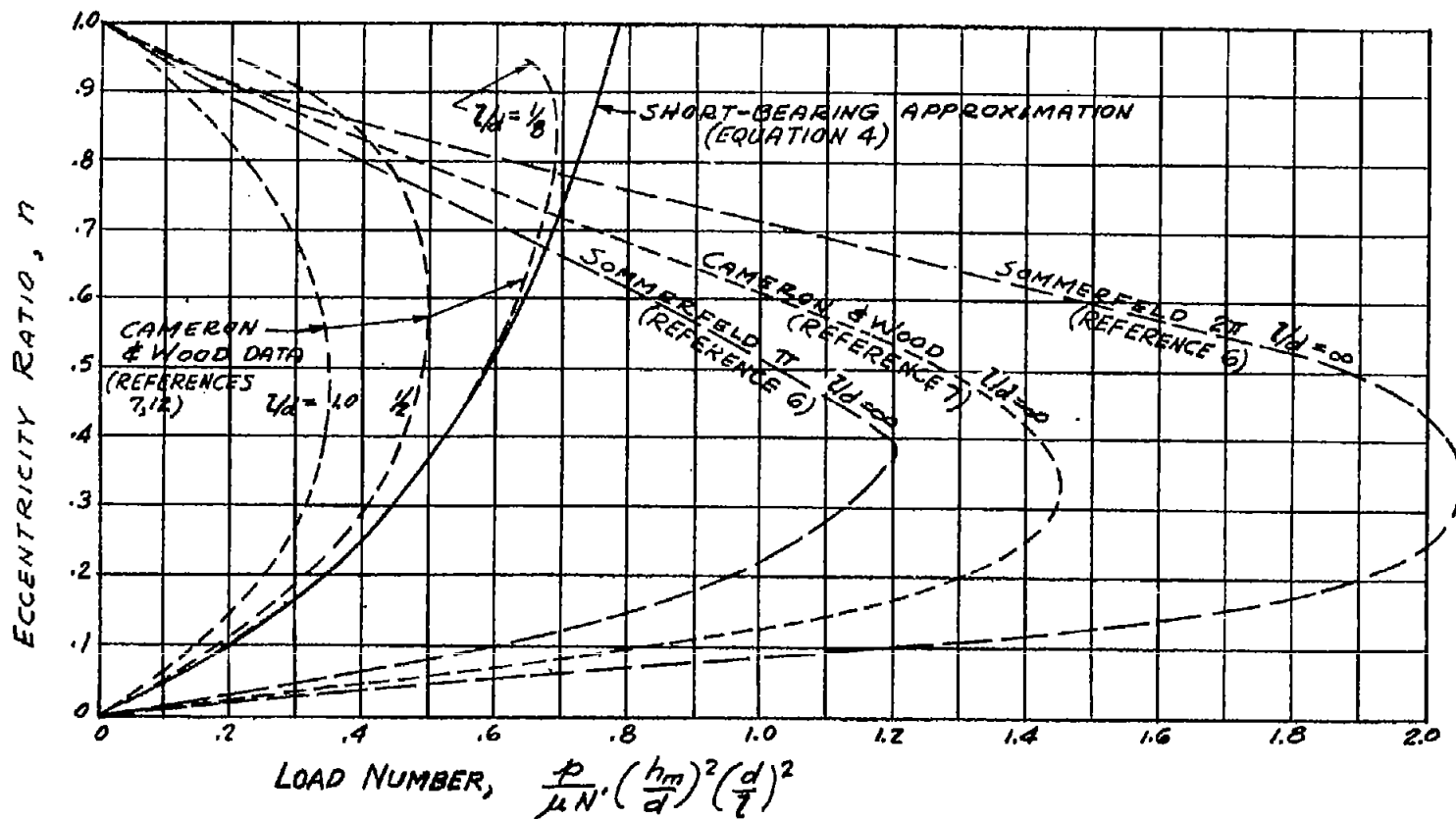
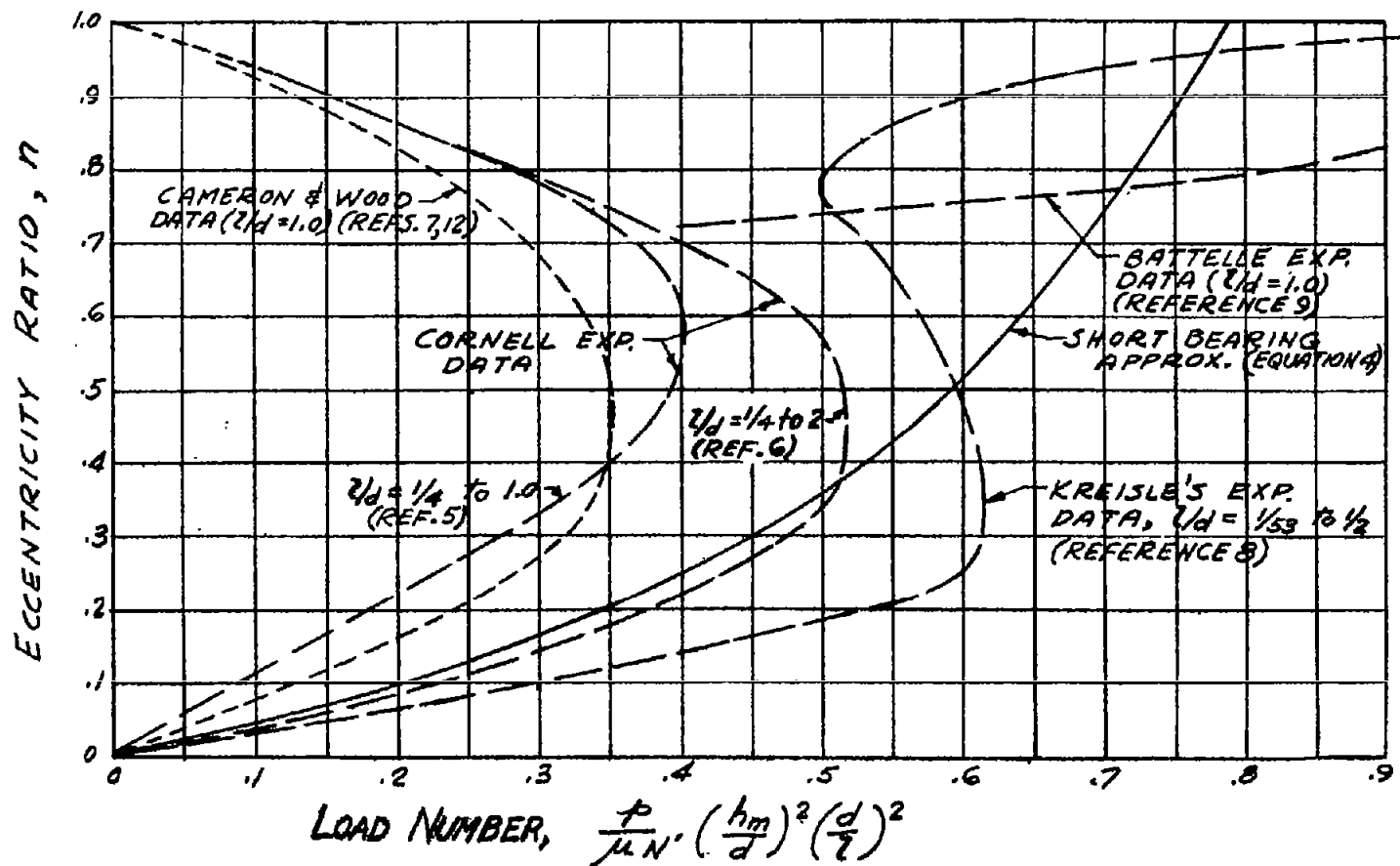


Figure 8.- Analytical curves from short-bearing approximation showing bearing load capacity against minimum film thickness on linear scales for comparison with figure 2. In ordinate scale, for $l/d > 1.0$ use $d/l = 1.0$.



(a) Comparison of various analytical curves.

Figure 9.- Comparison of various analytical and experimental curves using minimum film thickness instead of clearance as variable in load number. Near $n = 1.0$, product of p and h_m^2 in load number causes exaggerated effects. In abscissa scale, for $l/d > 1.0$ use $d/l = 1.0$.



(b) Comparison of experimental with analytical curves.

Figure 9.- Concluded.

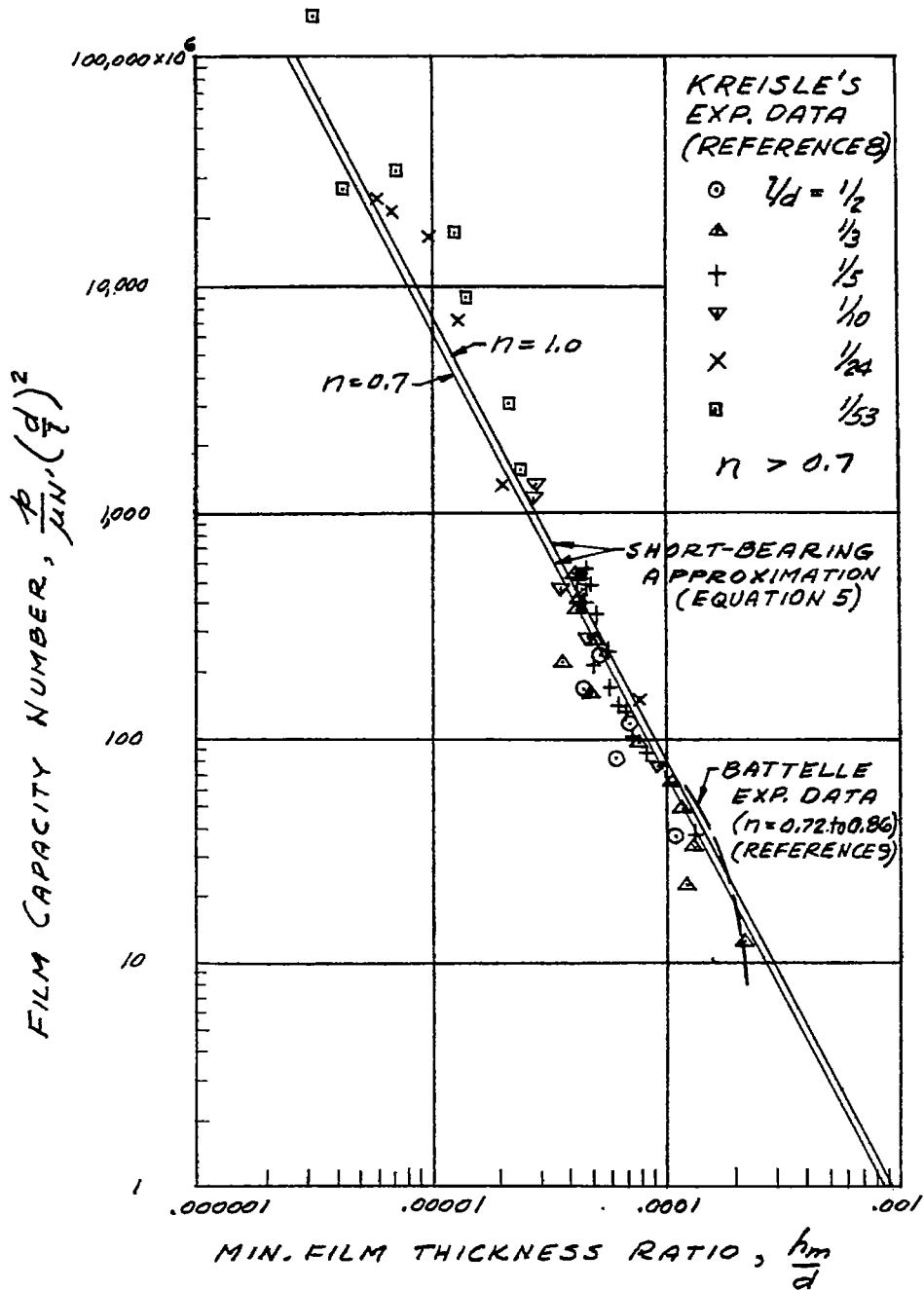


Figure 10.- Comparison of analytical curves from short-bearing approximation with Kreisle's experimental data at values of l/d from $1/2$ to $1/53$ (ref. 8). Battelle experimental curve (ref. 9) is also shown. Same data are also shown in figure 2.

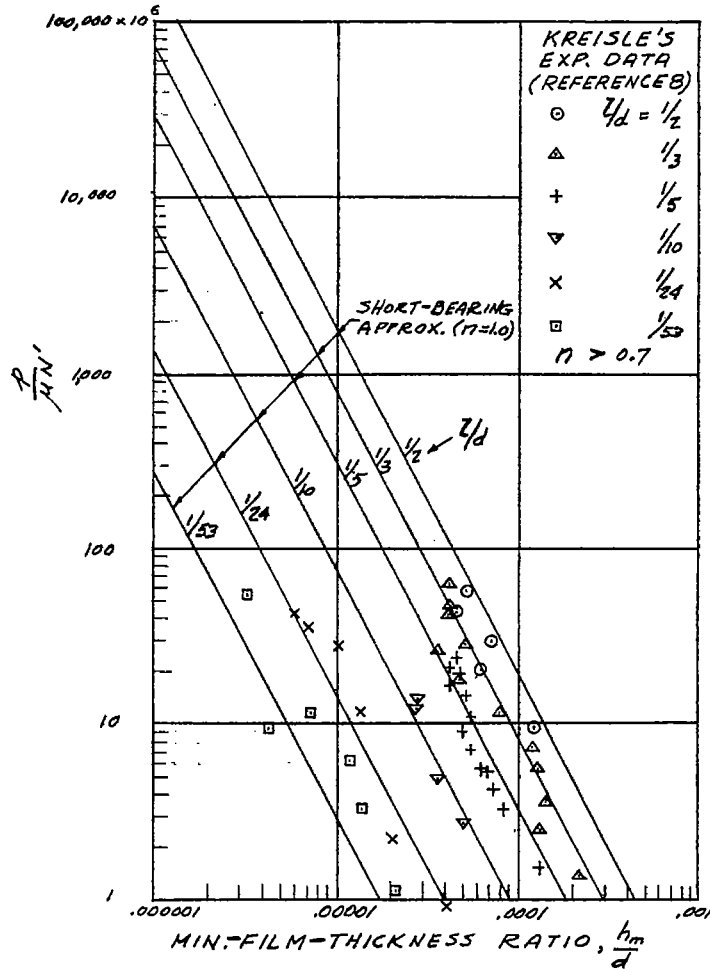


Figure 11.- Replot of Kreisle's experimental data (ref. 8) from figure 10 to show effect on film capacity number of omission of $(d/l)^2$ term for very short bearings.

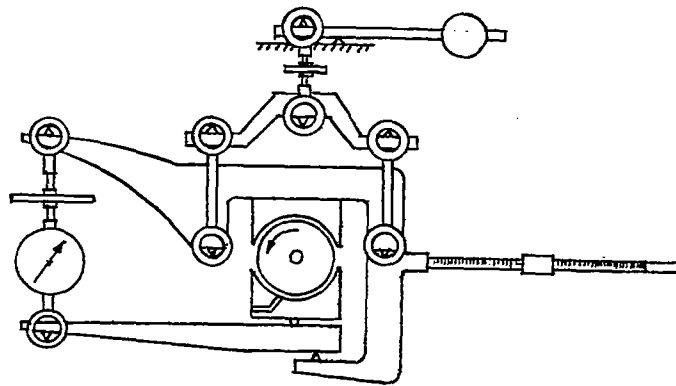


Figure 12.- Nutcracker-type bearing test machine used in reference 10.

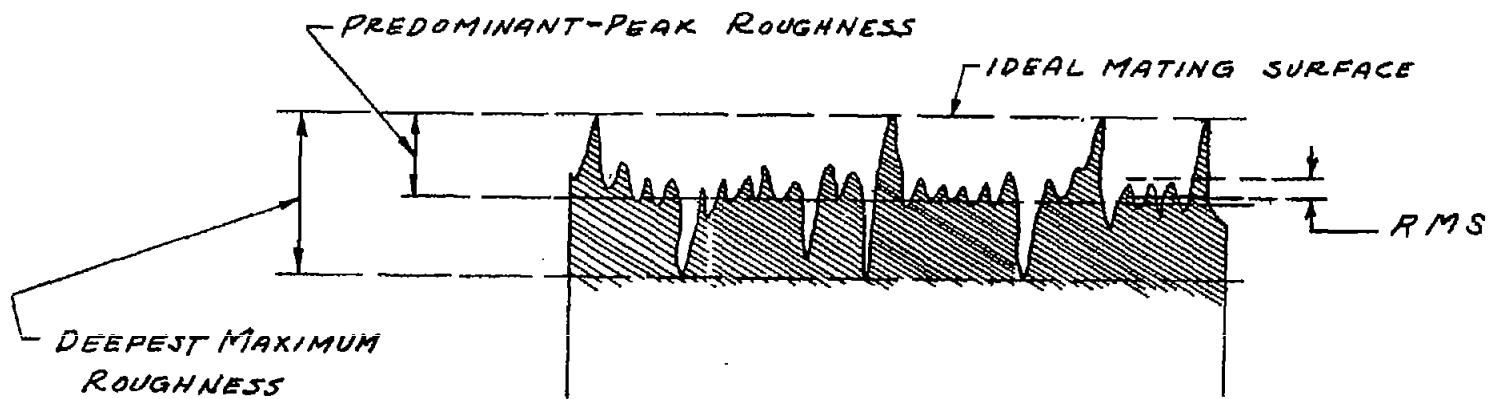


Figure 13.- Predominant-peak and deepest maximum roughnesses defined by Tarasov (ref. 11) as measures of surface roughness which are several times greater than measured root-mean-square values.

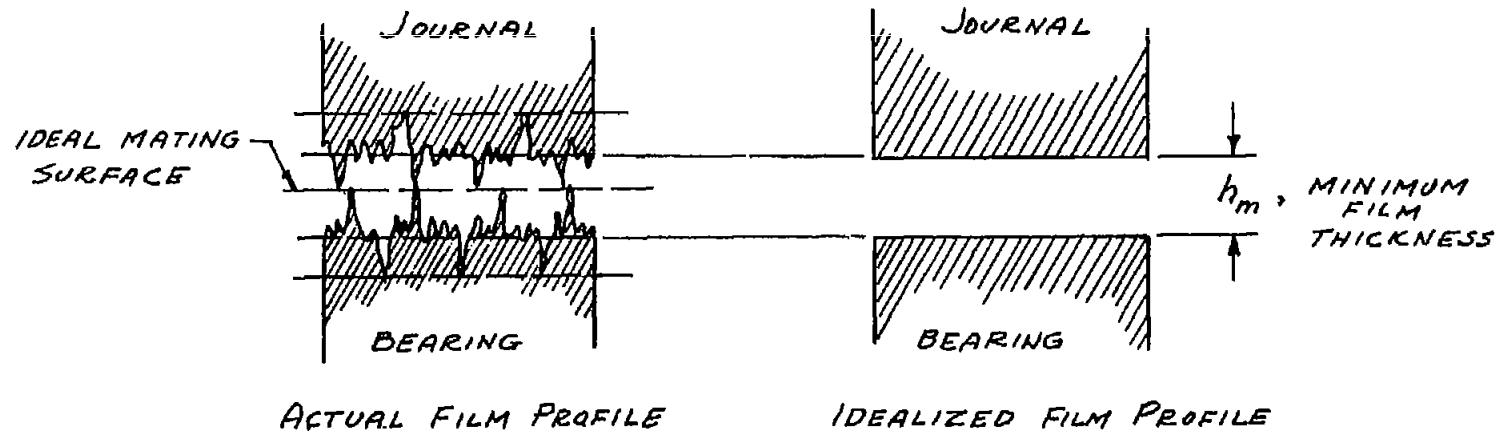


Figure 14.- Idealization of profile of minimum film at condition of minimum friction coefficient when peaks of journal surface are just at contact with peaks of bearing surface.

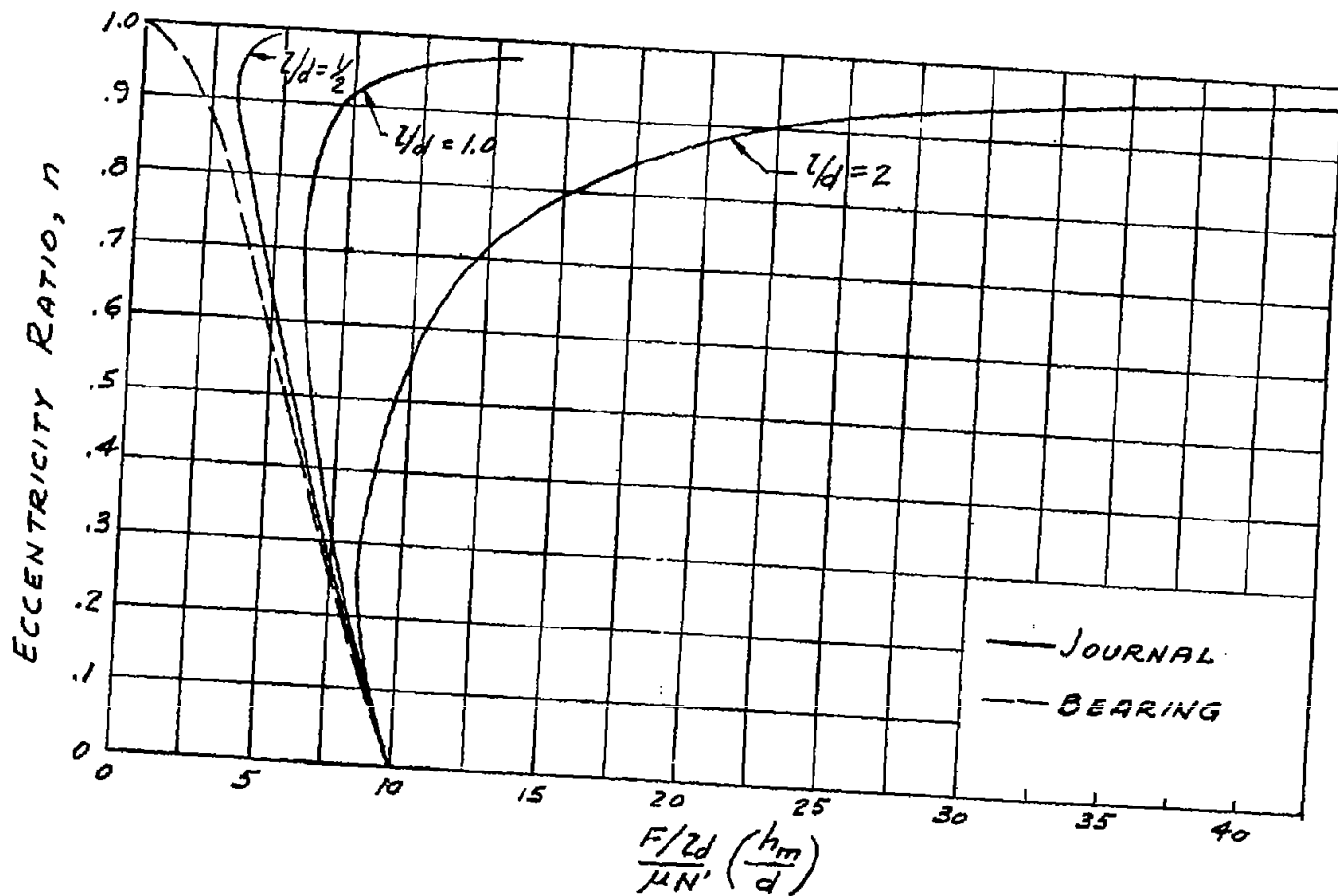


Figure 15.- Analytical curves from short-bearing approximation showing influence of eccentricity ratio on product of friction number and minimum-film-thickness ratio. (See eq. (16).)

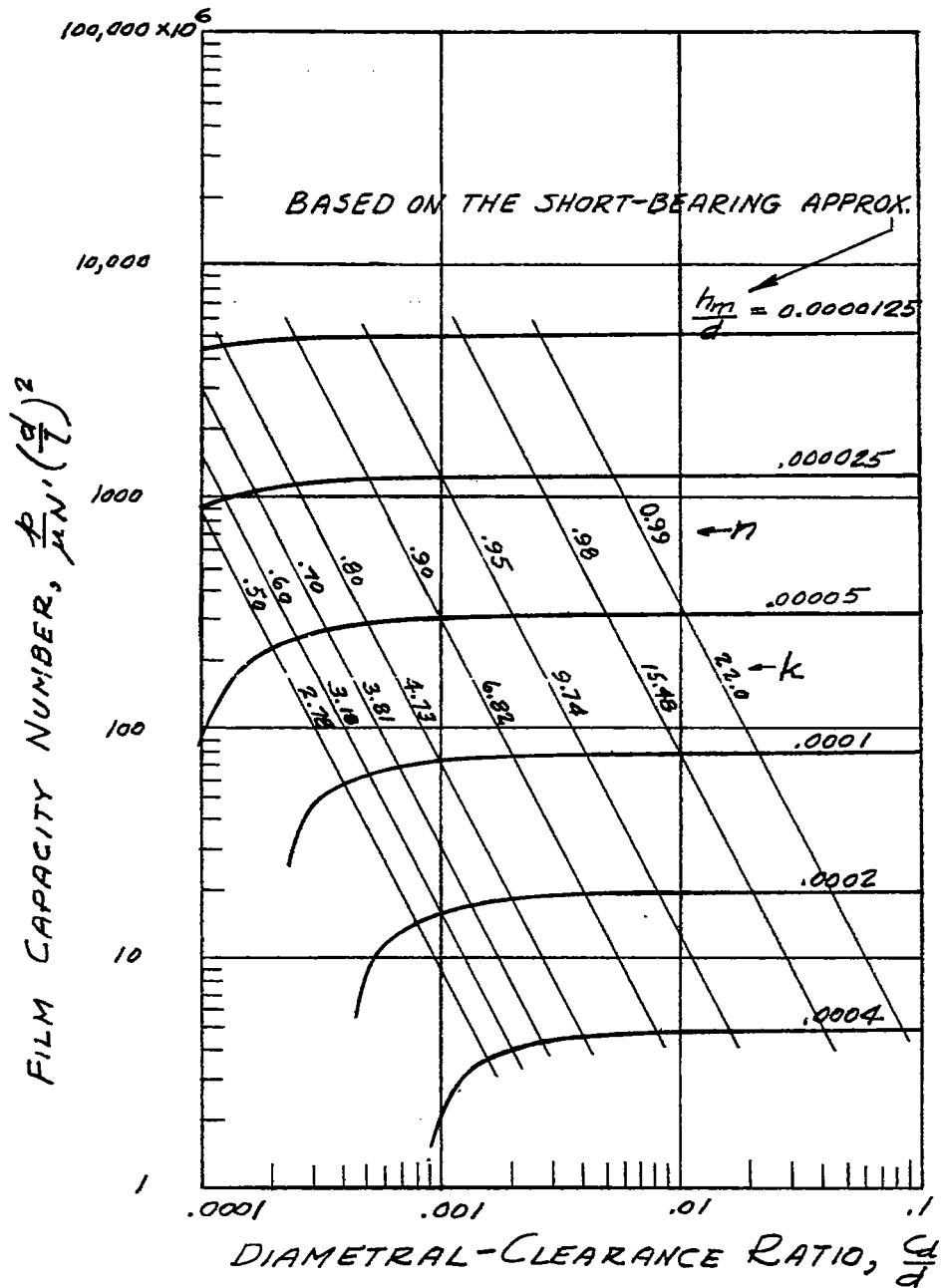


Figure 16.- Analytical curves showing effect of bearing-clearance changes on eccentricity ratio n and peak-pressure ratio k . (See fig. 3(a).) Peak-pressure ratio is ratio of magnitude of local oil-film pressure to unit load.

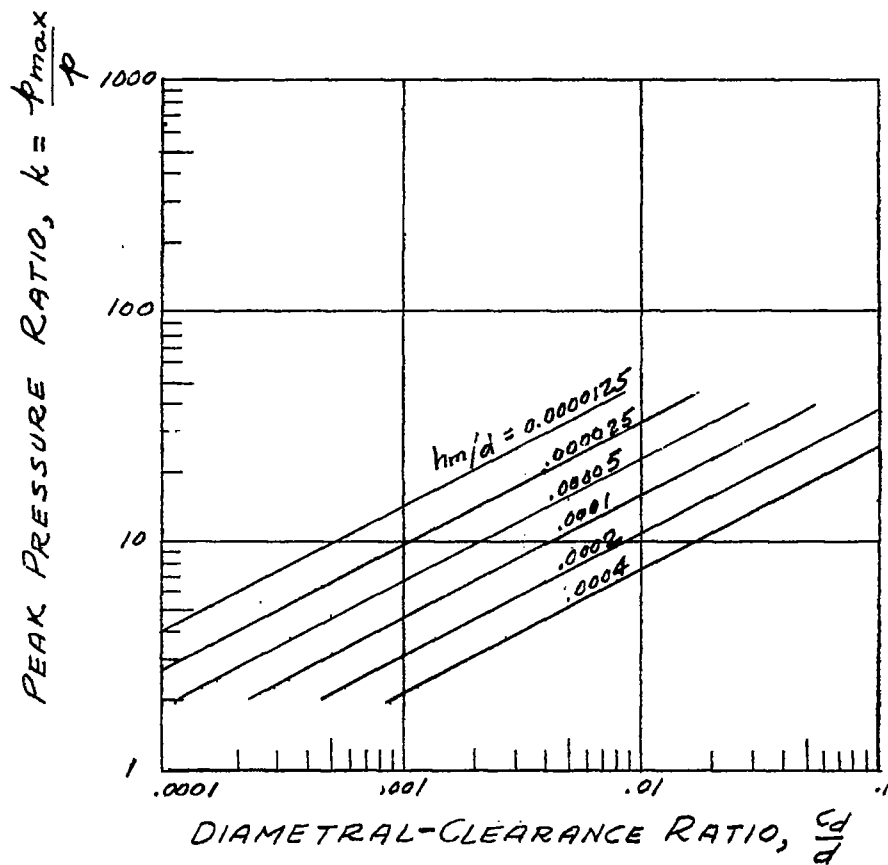


Figure 17.- Peak-pressure ratio shown as a function of clearance and minimum film thickness based on short-bearing approximation.